Concentrations, Particle-Size Distributions, and Dry Deposition Fluxes of Aerosol Trace Elements over the Antarctic Peninsula in Austral Summer

Songyun Fan[1], Yuan Gao[1], Robert M. Sherrell[2], Shun Yu[1], Kaixuan Bu[2]

[1]Department of Earth and Environmental Sciences, Rutgers University, Newark, 07102, USA
[2]Department of Marine and Coastal Sciences, Rutgers University, New Brunswick, 08901, USA

Correspondence to: Yuan Gao (yuangaoh@newark.rutgers.edu)

Abstract. Size-segregated particulate air samples were collected during the austral summer of 2016-2017 at Palmer Station on the Anvers Island, West Antarctic Peninsula, to characterize trace elements in aerosols. Trace elements in aerosol samples, including Al, P, Ca, Ti, V, Mn, Ni, Cu, Zn, Ce, and Pb, were determined by total digestion and sector field inductively coupled plasma mass spectrometer (SF-ICP-MS). The crustal enrichment factors (EF_{crust}) and k-means clustering results of particle size distributions show that these elements are derived primarily from three sources: (1) regional crustal emissions, including possible resuspension of soils containing biogenic P, (2) long-range transport, and (3) sea-salt. Elements derived from crustal sources (Al, P, Ti, V, Mn, Ce) with EF_{crust}<10 were dominated by the coarse-mode particles (>1.8 μm) and peaked around 4.4 μm in diameter, reflecting the regional contributions. Non-crustal elements (Ca, Ni, Cu, Zn, Pb) showed EF_{crust}>10. Aerosol Pb was primarily dominated by fine-mode particles, peaking at 0.14 - 0.25 μm, and likely was impacted by air masses from southern South America based on air-mass back trajectories. However, Ni, Cu, and Zn were not detectable in most size fractions and didn't present clear size patterns. Sea-salt elements (Ca, Na^+, K^+) showed a single-mode distribution and peaked at 2.5–4.4 μm. The estimated dry deposition fluxes of mineral dust for the austral summer, based on the particle size distributions of Al measured at Palmer Station, ranged from 0.65 to 28 mg m^{-2} yr^{-1} with a mean of 5.5 ± 5.0 mg m^{-2} yr^{-1}. The estimated dry deposition fluxes of the target trace elements in this study were lower than most fluxes reported previously for coastal Antarctica and suggest that atmospheric input of trace elements through dry deposition processes may play a minor role in determining trace element concentrations in surface seawater over the continental shelf of the West Antarctic Peninsula.

1 Introduction

Aerosols affect the climate through direct and indirect radiative forcing (Kaufman et al., 2002). The extent of such forcing depends on both physical and chemical properties of aerosols, including particle size and chemical composition (Pilinis et al., 1995). Size and chemical composition of aerosols influence aerosol optical properties as well as cloud formation and development (Weinzierl et al., 2017), and such information is critically needed in climate model for better estimating aerosol climate effects (Adebiyi and Kok, 2020). In the atmosphere, the removal of aerosols involves gravitational settling, impaction, diffusion, hygroscopic growth, and scavenging by precipitation, and the rates of all these processes are dependent on the aerosol particle size (Saltzman, 2009). Over the Southern Ocean and Antarctica, aerosol particle size distributions have been

studied (Gras, 1995; Järvinen et al., 2013; Xu et al., 2013; Kim et al., 2017; Herenz et al., 2019; Lachlan-Cope et al., 2020). Seasonal variations of the particle number concentrations were observed in the King Sejong Station, Antarctic Peninsula, and Halley Research Station on the Brunt Ice Shelf. The maximum and minimum of the particle number concentrations at two sites were found in the austral summer and austral winter, respectively (Kim et al., 2017; Lachlan-Cope et al., 2020). Due to the low background concentrations of aerosol particles, new particle formation has been suggested to substantially affect the annual aerosol concentration cycles (Lachlan-Cope et al., 2020). However, most of these studies focused on the physical characterises of aerosol particle size; the size distributions of aerosol trace elements are still poorly understood, and at present only aerosol Fe has been characterized for particle-size distributions around Antarctica (Gao et al., 2013, 2020).

Atmospheric aerosol deposition delivers nutrient elements to the open ocean, playing an essential role in maintaining marine primary production (Jickells and Moore, 2015; Jickells et al., 2016; Mahowald et al., 2018). A significant source of atmospheric trace elements in the remote oceans is continental dust derived from arid and unvegetated regions (Duce and Tindale, 1991). In addition, sea salt emission, volcanic eruptions, biomass burning, anthropogenic activities and even glacial processes contribute trace elements to the atmosphere (Pacyna and Pacyna, 2001; Chuang et al., 2005; Guieu et al., 2005; Crusius et al., 2011; Baker et al., 2020). The surface concentrations of the trace elements Al, Fe, Mn, Zn, and Pb in several open ocean regions depend strongly on atmospheric inputs (Duce et al., 1991; Prospero et al., 1996; Wu and Boyle, 1997; Measures and Vink, 2000; Moore et al., 2013; Bridgestock et al., 2016).

Atmospheric trace elements over the Southern Ocean and Antarctica may derive from distant continental sources through long-range transport (Li et al., 2008) and local dust sources in certain areas (Kavan et al., 2018; Delmonte et al., 2020). A wide range of aerosol studies has been carried out in Antarctica, with the intention of understanding the processes affecting aerosols and the background level of trace elements in the atmosphere (Zoller et al., 1974; Dick and Peel, 1985; Tuncel et al., 1989; Artaxo et al., 1990; Lambert et al., 1990; Dick, 1991; Artaxo et al., 1992; Loureiro et al., 1992; Mouri et al., 1997; Mishra et al., 2004; Arimoto et al., 2008; Gao et al., 2013; Xu and Gao, 2014; Winton et al., 2016). In the Antarctic Peninsula, the concentrations of aerosol trace elements were measured at several sites (Dick, 1991; Artaxo et al., 1992; Mishra et al., 2004; Préndez et al., 2009). Total dust deposition in this region was also estimated based on the ice-core record (McConnell et al., 2007). However, the measurement of particle size distribution of aerosol trace elements in Antarctic Peninsula is missing and there is no direct measurement that evaluated the importance of atmospheric deposition as a source of nutrients for primary producers in West Antarctic Peninsula shelf waters. Over the past several decades, one of the most dramatically warming regions in the Southern Hemisphere has been the Antarctic Peninsula (Vaughan et al., 2003; Bromwich et al., 2013; Turner et al., 2014). Warming ocean waters have caused most glaciers on the Peninsula to retreat (Cook et al., 2016) and small increases in air temperature are contributing to rapid summer melting and ice loss in this region (Abram et al., 2013).

Under conditions of low precipitation (Van Lipzig et al., 2004) and high wind speed (Orr et al., 2008), several ice-free areas on James Ross Island, off the east coast of the northern Peninsula could serve as local dust sources (Kavan et al., 2018), and such sources may contribute to the atmospheric loading of certain trace elements such as Fe (Winton et al., 2014; Gao et al., 2020). Similar ice-free areas were found in King George Island, Livingston Island, Anvers Island etc. in the Antarctic

Peninsula region (Bockheim et al., 2013), and may act as potential sources of aeolian dust. As part of the current study, the particle size distribution of aerosol Fe measured at Palmer Station showed single mode distribution and was dominated by coarse particles, suggesting that local regional dust emission dominated the concentration of Fe in this region (Gao et al., 2020). Under the current warming trend, ice core data show that lithogenic dust deposition more than doubled during the 20th century in the Antarctic Peninsula (McConnell et al., 2007). In addition, the rapid warming condition may enhance the emission of other sources. For example, the Antarctic Peninsula has been suggested as one of the sites that have the highest P excretions contributed by seabird colonies globally (Otero et al., 2018). The enhanced local dust emission may thus cause an increased P emission as well. Consequently, dust emissions induced by regional warming may have impacted the concentrations of aerosol trace elements in the marine atmosphere over the Antarctic Peninsula, affecting atmospheric deposition of trace elements to coastal waters off the Antarctic Peninsula and adjacent pelagic waters of the Southern Ocean (Wagener et al., 2008). However, aerosol trace elements are still under-sampled around coastal Antarctica, and thus quantification of the chemical and physical properties of aerosols and accurate estimation of the atmospheric deposition of trace elements to the region are inadequate.

This study presents multi-element results from an *in-situ* measurement of size-segregated aerosol particles at Palmer Station, Antarctic Peninsula, in the austral summer of 2016–2017. The objectives are to (1) measure the concentrations and size distributions of a suite of aerosol trace elements, (2) determine potential sources of the elements, and (3) estimate dry deposition fluxes of the elements based on the concentrations in ten size classes of aerosols. Results from this study fill a data gap critically needed for characterization of aerosol properties and for improving quantification of the fluxes that contribute to regional biogeochemical cycles. The new observational data also provide insight into sources of aerosol trace elements, as influenced recently by warming, which exposes a greater area of ice-free land, and by the impact of human activities in this region. A full discussion of atmospheric Fe in this sample set was published recently (Gao et al., 2020); this paper extends that study by investigating the concentrations, size distributions, and dry deposition fluxes of a suite of additional aerosol trace elements.

2 Methods

2.1 Sampling and sample treatment

Aerosol size-segregated samples were collected during austral summer from November 19, 2016 to January 30, 2017 at Palmer Station (64.77° S, 64.05° W, Figure 1), located on the southwestern coast of Anvers Island off the Antarctica Peninsula. A detailed description of the aerosol sampling, including the protocols for mitigating contamination in the pristine environmental can be found in Gao et al. (2020). Briefly, sampling was conducted using a ten-stage Micro-Orifice Uniform Deposit Impactor^{TM} (MOUDI, MSP Corp., MN, USA) with a 30 L min^{-1} flow rate. The 50% cut-off aerodynamic diameters of MOUDI are 0.056, 0.10, 0.18, 0.32, 0.56, 1.0, 1.8, 3.2, 5.6, 10, and 18 μm. In this study, size fractions ≤1.0 μm were summed to operationally define fine-mode particles and those ≥1.8 μm were summed to define coarse-mode particles, similar to previous studies which operationally divided aerosol particles into fine and coarse fractions using a cut-off size of 1.0–3.0 μm (Siefert

et al., 1999; Chen and Siefert, 2004; Buck et al., 2010; Gao et al., 2019). The aerosol sampler was placed on a sampling platform which was ~300 m east from the station center and ~3 m high above the ground (~20 m above sea-level) in "Palmer's backyard" (Gao et al., 2020). To avoid local contamination from the research station, a wind control system was set up to pause aerosol sampling when wind direction was inside the sector ±60° from the direction of the station buildings or when wind speed <2 m s^{-1}. The active sampling time was about 71-98% of the total sampling time (Table 1). Due to extremely low concentrations of aerosol trace elements over Antarctica, the duration of each sampling event was approximately one week (Table 1).

After each sampling, the MOUDI sampler was carried back to the lab in the research station for sample filter changing and sampler cleaning in a Class 100 cleanroom flow bench. Aerosol samples were stored frozen in pre-cleaned Petri dishes at -20℃ before analyses. A total of 8 sets size-segregated aerosol samples were collected on Teflon filters (1 μm pore size, 47 mm diameter, Pall Corp., NY, USA). A full set of blank filters (n = 11) was mounted on the sampler, carried to the sampling platform without running the sampler, and thus defined as field blanks. Meteorological conditions were recorded *in situ* by a weather station (Campbell Scientific, UT, USA) installed on the same platform (Table 1).

2.2 Chemical analyses

2.2.1 Trace elements in aerosols

Aerosol samples were analyzed for the concentrations of trace elements by an Element-1 sector field inductively coupled plasma mass spectrometer (SF-ICP-MS, Thermo-Finnigan, Bremen, Germany) at the Department of Marine and Coastal Sciences of Rutgers University, following a strong-acid digestion method described in Gao et al. (2020). Elemental concentrations were determined for Al, P, Ca, Ti, V, Mn, Ni, Cu, Zn, Ce, and Pb. Briefly, a quarter of each sample filter was digested in a closed 15 mL Teflon vial (Savillex, MN, USA) with Optima Grade HF (0.1 mL) and HNO_3 (0.8 mL) (Fisher Scientific, NJ, USA). Sample digestion was performed on a uniform heating HPX-200 (Savillex, MN, USA) hot plate for 4 hours at 165 ℃ followed by complete evaporation of acids. Then, 2.0 mL 3% HNO_3 with 1 ppb Indium (In) solution was added to re-dissolve the sample, the In used as an internal standard to correct instrument drift in the ICP-MS analyses. All the digestion processes were carried out in a HEPA filter-controlled Class 100 clean hood in the Atmospheric Chemistry laboratory at Rutgers University. The Teflon vials and test tubes used in this study were thoroughly acid-cleaned. To ensure the data quality, for each batch of samples, at least two procedural blanks were processed in the same way as the samples to monitor for possible contamination. During the ICP-MS analysis, duplicate injections of sample solutions were made every ten samples to check the instrument precision (Table S1). The recovery of this analytical protocol was estimated by 7 separate digestions of the Standard Reference Material (SRM) 1648a-urban particulate matter (National Institute of Standard and Technology, MD, USA) (Table S1). The method limits of detection (LOD) were calculated as three times the standard deviation of 11 field blanks and a 200 m^3 representative sampling volume (Table S1). The medians of %blank in samples for detectable trace elements were calculated for quality control (Table S1). The concentrations below LOD were given a concentration of zero

for the purposes of this study. Elements with all concentrations lower than the LOD, including Cr, Co, Cd and Sb, were measured but are not reported or discussed. The aerosol Fe concentrations were reported in Gao et al. (2020) and are not included in this paper. Although the fractional solubility of Fe was obtained, the solubilities for the other trace elements are not measured or discussed in this study.

2.2.2 Ionic tracers in aerosols

The concentrations of water-soluble Na^+ and K^+ in aerosols were analyzed by ion chromatography (IC) (ICS-2000, Dionex, CA, USA) with an IonPac CS12A (2 × 250 mm^2) analytical column at the Atmospheric Chemistry laboratory at Rutgers University. The cations Na^+ and K^+ were used as tracers to estimate the portion of aerosols derived from seawater and biomass burning, respectively. The non-sea-salt K^+ (nss-K^+) was estimated using the equation: $[nss\text{-}K^+] = [K^+] - 0.037[Na^+]$. Sample processing for IC analysis was similar to the method used by Zhao and Gao (2008) and Xu et al. (2013). Briefly, a quarter of the sample filter was transferred to a plastic test tube and leached with 5.0 mL Milli-Q water in an ultrasonic bath for 20 minutes at room temperature. Before being injected into the IC, the leachate was filtered through a PTFE syringe filter (0.45 μm pore size, VWR, PA, USA). The method LODs for Na^+ and K^+ based on 7 blanks and a 200 m^3 representative sampling volume were 2 and 1 ng m^{-3}, respectively. The precision of the analytical procedures based on seven spiked samples was <±1%.

2.3 Data analyses

2.3.1 Enrichment factors

To achieve an initial estimate of the possible sources for trace elements, enrichment factors relative to upper continental crust (EF_{crust}) were calculated, using the equation:

$$EF_{crust} = \frac{(X_i/X_{Al})_{sample}}{(X_i/X_{Al})_{crust}} \quad (1)$$

where $(Xi/X_{Al})_{sample}$ is the mass concentration ratio of element i to the crustal reference element, Al, in aerosol samples, and $(Xi/X_{Al})_{crust}$ is the abundance ratio of element i to Al in the upper continental crust (Taylor and McLennan, 1995). The crustal reference element Al has been widely used to calculate crustal enrichment factors in the Southern Ocean and Antarctica (Zoller et al., 1974; Dick, 1991; Lowenthal et al., 2000; Xu and Gao, 2014). When the EF_{crust} is greater than 10, the element likely has additional contributions from other sources (Weller et al., 2008).

2.3.2 Particle size distribution and k-means clustering

The aerosol particle size distributions were converted to normalized concentrations which is defined as the concentration of trace elements in a size bin divided by the width of the bin (Warneck, 1988):

$$\frac{dC}{d\log(D_p)} = \frac{dC}{\log(D_{p,u}) - \log(D_{p,l})}$$

In the equation, dC is the mass concentration of trace elements in a size bin, and $d\log(D_p)$ is the difference in the log of the bin width. The $d\log(D_p)$ is calculated by subtracting the log of the lower bin boundary ($\log(D_{p,u})$) from the log of the upper bin boundary ($\log(D_{p,l})$). The k-means clustering algorithm was used to cluster the average particle size distribution of each trace element. The optimal number of clusters (k) was selected by choosing the k with the highest Calinski-Harabasz index (Caliński and Harabasz, 1974).

2.3.3 Atmospheric dry deposition flux estimation

Dry deposition flux (F_d, mg m^{-2} yr^{-1}) of each element in aerosols was calculated from the concentration (C_e, ng m^{-3}) of the trace element in the air and dry deposition velocity (V_d, cm s^{-1}):

$$F_d = 0.315 \times V_d \times C_e \quad (2)$$

where 0.315 is a unit conversion factor (Gao et al., 2013). The V_d for each trace element was computed by dry deposition rates (V_{di}, cm s^{-1}) and particle distribution ratios (P_{dri}, %) following the equation:

$$\sum_{i=1}^{10} V_{di} \times P_{dri} (3)$$

The P_{dri} was derived from the concentrations of trace elements in different size fractions i and V_{di} was estimated using a combination model of Williams (1982) and Quinn and Ondov (1998). This model includes the effects of wind speed, air/water temperature difference, sea surface roughness, spray formation in high wind speed and relative humidity. Meteorological parameters used for estimating dry deposition rates were measured *in situ* by the weather station with 1 minute temporal resolution that was converted to 1 hour averages. Sea surface temperature data were obtained from the Palmer Station Long-Term Ecological Research (LTER) study (https://oceaninformatics.ucsd.edu/datazoo/catalogs/pallter/datasets/28). Dry deposition rates of coarse-mode particles were dominated by gravitational settling, whereas the dry deposition rates of smaller particles were controlled by environmental factors, including wind speed, relative humidity, air temperature, and sea surface temperature (Figure 2). Therefore, the uncertainties of the dry deposition velocity estimation for the elements that were dominated by coarse particles were about ±30-60%, and the uncertainty of fine particle dominated element (Pb) was about ±100%. The overall estimation of dry deposition flux usually carries substantial uncertainty (a factor of 2 to 4) due to the limited sampling volume and the assumptions inherent to the V_{di} estimation (Duce et al., 1991; Gao et al., 2020). The dry deposition velocities determined for each element are reported in Table 3. Dry deposition fluxes were calculated for the trace elements showing clear particle size distribution patterns: Al, P, Ca, Ti, V, Mn, Ce, and Pb. For Ni, Cu, and Zn, that didn't show clear size distributions, the ranges of their dry deposition fluxes were also estimated by applying their mean concentrations to the lowest (Pb, 0.11 ± 0.12 cm s^{-1}) and highest (Al, 0.49 ± 0.28 cm s^{-1}) dry deposition velocities. The dry deposition fluxes of dust were estimated based on the concentrations and particle size distributions of Al in aerosols, assuming that Al accounted for 8% of dust mass (Taylor and McLennan, 1995).

2.3.4 Air mass back trajectories

To explore possible source regions of air masses affecting trace elements in aerosols collected at Palmer Station, the NOAA Hybrid Single Particle Lagrangian Integrated Trajectory Model (HYSPLIT) was used to calculate 72-hour air mass back trajectories for each sampling duration (Rolph et al., 2017). In this study, the HYSPLIT model was driven by the meteorological data from the Global Data Assimilation System (GDAS) with a 0.5-degree resolution. Each air mass back trajectory was calculated at 3-hour intervals and started from one-half mixed boundary layer height. The back trajectories during each sampling period were used to calculate trajectory frequencies which were defined by the following equation:

$$\text{Trajectory frequencies} = 100 \times \frac{\text{number of endpoints per grid square}}{\text{number of trajectories}} \quad (4)$$

3 Results and discussion

3.1 Enrichment factors of trace elements

Crustal enrichment factors of trace elements in aerosols were calculated as the first step of source identification (Figure 3). Two major EF groups were found, representing crustal and non-crustal elements as follows.

3.1.1 Crustal elements (P, Ti, V, Mn, Ce)

The values of EF_{crust} for Ti, V, Mn, and Ce in aerosol samples were less than 10, indicating that a crustal source is the dominant source for those elements (Figure 3). As typical lithogenic elements (Boës et al., 2011), Ti and Mn in aerosols over oceanic regions are usually derived from natural dust emissions (Shelley et al., 2015; Marsay et al., 2018; Buck et al., 2019). Likewise, V and Ce in aerosols over the South Pole were reported dominated by crustal weathering (Zoller et al., 1974). In addition to crustal emissions, long-range transport may deliver some portion of these trace elements from remote sources to Antarctica (Wagener et al., 2008). For example, aerosol Ce and Mn derived from anthropogenic emissions were thought to be contributed by additives in vehicle fuels (Fomba et al., 2013; Gantt et al., 2014), and V in aerosols was found associated with ship emissions due to the use of heavy oil fuel (Keywood et al., 2020). However, the EF_{crust} results from this study suggest that nearby fuel combustion did not cause significant enrichment of V in aerosols at Palmer Station. Similarly, unenriched V was observed at McMurdo Station where light-weight fuel oil was used that was not a significant source of V (Lowenthal et al., 2000). We conclude that Ti, Mn, V, and Ce observed at Palmer Station were derived primarily from crustal sources.

The range of EF_{crust} for P was between 2 and 8, relatively higher than that of the other crustal elements. In Antarctic soils, P has been widely studied (Campbell and Claridge, 1987; Blecker et al., 2006; Prietzel et al., 2019). Around the Antarctic coast, including the northern end of the Antarctic Peninsula, high P inputs to the surface soil were found in seabird colonies (Otero et al., 2018), and a high enrichment of P (EF_{crust} = 33) was reported previously at King George Island (Artaxo et al., 1990). The closest potential source, the penguin colony on Torgerson Island, is only about 1 km from Palmer Station. Given that regional wind-induced dust likely affects aerosol composition over the Antarctic Peninsula (Asmi et al., 2018; Gao et al.,

2020), soil-derived P is likely to be emitted to the atmosphere. In addition, biogenic activities in Antarctica also produce abundant gaseous P, such as phosphine, through anaerobic microbial processes in soils and animal digestives, and phosphine gas can be transformed to other low-volatile P-containing compounds in the atmosphere or soils (Zhu et al., 2006). Primary biogenic aerosols, sea-salt aerosols, and volcanic emissions could also contribute P to the atmosphere, causing an elevated EF_{crust} for P (Zhao et al., 2015; Trabelsi et al., 2016).

3.1.2 Non-crustal elements (Ca, Ni, Cu, Zn, Pb)

The enrichment factors of atmospheric Ni, Cu, Zn, and Pb relative to the crustal element Al, were found to be greater than 10 in some samples, suggesting contributions from non-crustal sources during the corresponding sampling periods in this study (Figure 3). High enrichments of these elements in Antarctica have commonly been associated with long-range transport derived from anthropogenic emission (Boutron and Lorius, 1979; Maenhaut et al., 1979; Dick, 1991; Artaxo et al., 1992; McConnell et al., 2014; Xu and Gao, 2014). Aerosol Cu, Zn, and Pb are contributed primarily by combustion or industrial activities (Pacyna and Pacyna, 2001). Strong variations of the EF_{crust} of Cu, Zn, and Pb observed in snow samples at Dome C, Antarctica, over the 20th century, were attributed to volcanic activities (Boutron and Lorius, 1979). On the other hand, heavy oil combustion was found to be the major source of aerosol Ni and V, and V/Ni ratios are usually used to identify shipping emissions (Keywood et al., 2020). Nevertheless, the V/Ni measured at Palmer Station ranged from 0.01 to 0.2, much lower than the V/Ni = 3.2 ± 0.8 characteristic of the discharge from ship engines (Viana et al., 2009; Viana et al., 2014; Celo et al., 2015). Hence, despite the recent increase in tourist ship traffic (Lynch et al., 2010), it seems that Palmer Station was barely impacted by ship emissions, which is consistent with the EF_{crust} of V. As a common crustal element, Ca accounts for about 3.5% of the weight of Earth's crust (Taylor and McLennan, 1995), while Ca is also a conservative major ion in seawater (Millero, 2016). The high EF_{crust} for Ca at Palmer Station suggests that aerosol Ca was mainly derived from sea-salt.

3.2 Concentrations of trace elements

The concentrations of Ca and Al, the two major elements measured in this study, were one to several orders of magnitude higher than other elements (Table 1). To place all of the results of this study into the context of past investigations, we provide a visual comparison of measured concentrations of aerosol trace elements over Antarctica (Figure 4).

3.2.1 Mineral dust (Al, P, Ti, V, Mn, Ce)

The concentrations of Al in aerosols varied from 1.2 to 7.9 ng m^{-3} with an average of 4.3 ng m^{-3} during 2016-2017 austral summer in this study. These concentrations are lower than the 4-year mean Al values of ~13 ng m^{-3} at King George Island (62° S, 58° W), at the northern end of the Antarctic Peninsula (Artaxo et al., 1992), but were slightly higher than the 2-year mean Al concentrations of 1.9 ng m^{-3} observed at King Sejong Station (62° S, 59° W) (Mishra et al., 2004), the summer mean of 0.194 ng m^{-3} at Larson Ice Shelf to the southeast of Palmer Station (Dick et al., 1991), the 5-year summer mean of 1.3 ng m^{-3}

in East Antarctica (Weller et al., 2008) and the summer average of 0.57 ng m^{-3} measured at the South Pole (Zoller et al., 1974; Maenhaut et al., 1979) (Figure 4b). All these results, including ours, were much lower than the average Al concentrations of 180 ng m^{-3} and 250 ng m^{-3} observed on the two sites at McMurdo Station (Mazzera et al., 2001) due to the impact of the McMurdo Dry Valleys (Figure 4b). The nearby McMurdo Sound was reported as the dustiest site in Antarctica (Winton et al., 2016). These aerosol Al concentrations are also lower than the average Al concentration 190 ng m^{-3} observed in coastal East Antarctica where the samples were also impacted by air masses passing over McMurdo regions (Xu and Gao, 2014) (Figure 4b). The concentrations of Ti ranged from 140 to 800 pg m^{-3} with an average of 250 pg m^{-3}, while the concentration of Mn ranged from 17 to 44 pg m^{-3} with an average of 30 pg m^{-3}. Both Ti and Mn concentrations at Palmer Station were lower than yearly mean concentrations at King George Island (average Ti: 1600 pg m^{-3}, average Mn: 660 pg m^{-3}) (Artaxo et al., 1992), and they were also lower than the summer mean PM_{10} concentrations at McMurdo Station (Ti: 26000 pg m^{-3}, Mn: 3000 pg m^{-3}) (Mazzera et al., 2001). However, these Ti and Mn values observed at Palmer Station were in the same magnitude with the $PM_{2.5}$ concentrations during the austral summer near Chilean Bernardo O'Higgins base, located on the northwest coast of the Antarctic Peninsula (Préndez et al., 2009) and with the concentrations in bulk aerosols over coastal East Antarctica in austral summer (Mn: 450–1200 pg m^{-3} with an average of 700 pg m^{-3}) (Xu and Gao, 2014) (Figure 4e and g). The concentrations of V ranged from 2.7 to 6.1 pg m^{-3} with a mean value of 4.2 pg m^{-3}, which is higher than the numbers reported at the South Pole (average ~1.5 pg m^{-3}) (Zoller et al., 1974; Maenhaut et al., 1979) (Figure 4f). However, the V concentration observed at Palmer Station was much lower than previous observations in North Atlantic Ocean (50–3170 pg m^{-3}) (Fomba et al., 2013) and eastern Pacific Ocean (average 150 pg m^{-3}) (Buck et al., 2019). On the other hand, Ce demonstrated an average concentration of 1.3 ± 0.69 pg m^{-3}, which is consistent with the Ce concentrations reported at Neumayer Station, Antarctica (Weller et al., 2008) (Figure 4k). The low concentrations of aerosol V and Ce suggest that Palmer Station was not significantly influenced by fossil fuel combustion. The P concentrations in aerosols during this study ranged from 85 to 250 pg m^{-3} with an average of 150 ng m^{-3}. The concentrations of aerosol P at Palmer Station were lower than that at King George Island (3820 pg m^{-3}) (Artaxo et al., 1990). Comparing global aerosol P concentrations, we find that P concentrations over the Antarctic Peninsula are in the same range as those over the Central Pacific Ocean (Chen, 2004). In this study, nss-K^+ was used as a tracer of biomass burning (Winton et al., 2015). The calculated nss-K^+ was indistinguishable from zero, suggesting that K^+ in aerosol at Palmer Station was primarily derived from sea water, not from biomass burning through long-range transport. These results agree well with the air mass back trajectories, which indicate that most samples collected during this study were barely affected by South America (Figure 5). In addition, for most of the 72-hour air-mass back trajectories, the highest frequencies were found around the northern Antarctic Peninsula, suggesting that aerosol crustal elements observed at Palmer Station were impacted by sources in that region (Figure 5).

3.2.2 Anthropogenic aerosols (Ni, Cu, Zn, Pb)

The concentrations of Ni, Cu, Zn, and Pb in were more variable than the crustal elements. High levels of these elements would suggest an effect of a polluted air mass derived from long-transport or regional air pollution (Artaxo et al., 1992). The highest

concentration of Ni observed during this study was 320 pg m^{-3}, with an average of 75 pg m^{-3}, while the lowest Ni concentration was below LOD (<20 pg m^{-3}). Samples M2 and M10 showed relatively high values of Ni with 320 and 200 pg m^{-3}, respectively, while the concentrations of Ni in M1, M5, and M6 were much lower, ranging from 17 to 37 pg m^{-3}. The concentrations of Cu varied from <20–480 pg m^{-3} (average 150 pg m^{-3}), while Zn ranged from <30–710 pg m^{-3} (average 200 pg m^{-3}). These results indicate that the concentrations of these elements in aerosols varied dramatically throughout the study period, likely affected by the source strength and meteorological conditions. From the air mass back trajectories, the samples with high Ni (M2, M10), Cu (M1, M2, M4, M10) and Zn (M5) all were impacted by significant amount of air masses from the South Pacific Ocean and South America (Figure 5). The back trajectories of air masses of M7 didn't touch South America but the concentration of Zn in this sample was high. With the fact that aerosol Zn was found in both fine- and coarse-mode fractions (Table 2), both local sources and long-range transport may contribute to this element in the air. Artaxo et al. (1992) collected aerosol samples using a 2-stage size-segregated sampler and observed high concentrations of Ni, Cu, and Zn with averages of 240, 790 and 7200 pg m^{-3} at King George Island in summertime (Figure 4h, i and j), much higher than the results from this study. The high concentrations may have resulted from local polluted dust emissions around their sampling site (Hong et al., 1999). In addition, their sampling site was considerably north of Palmer Station, and may be more likely to be impacted by air masses from South America (Chambers et al., 2014). In South America, high enrichment of Ni, Cu, Zn, and Pb in fine-mode particles was reported to be primarily associated with vehicle emission, soil dust, and oil combustion (Artaxo et al., 1999; Jasan et al., 2009). Moreover, miming activities were suggested as an important source, especially in remote sites in South America (Carrasco and Préndez, 1991; Klumpp et al., 2000). On the other hand, the concentrations of Ni, Cu, and Zn at Palmer Station were lower than some other sites in Antarctica. At McMurdo Station, the average concentrations of Cu and Zn in PM_{10} samples were 200 and 1200 pg m^{-3} (Mazzera et al., 2001) (Figure 4i and j). Over coastal East Antarctica, the Ni concentrations in aerosols ranged from <3 to 2200 pg m^{-3} with an average of 750 pg m^{-3} (Xu and Gao, 2014) (Figure 4h).

The concentrations of aerosol Pb observed at Palmer Station ranged from 5.0 to 60 pg m^{-3} with an average of 19 pg m^{-3}, higher than the average concentration of 4.7 pg m^{-3} previously observed on the east coast of the Antarctic Peninsula in austral summer (Dick, 1991) (Figure 4l) and the annual average concentration of 11 pg m^{-3} in Tasmania (Bollhöfer et al., 2005). However, the average Pb concentration reported at King George Island was about 800 pg m^{-3} (Artaxo et al., 1992), considerably higher than observed in this study (Figure 4l). The two highest Pb concentrations observed during this study were in M4 (60 pg m^{-3}) and M5 (30 pg m^{-3}). The results of air mass back trajectories for M4 and M5 show that the air masses were derived in part from South America, which suggests additional contribution from long-range transport (Figure 5b and c). However, when the 72-hour air mass back trajectories did not intersect the South American continent, the concentrations of Pb in those samples were significantly lower (Figure 5a and d). The low concentrations of Pb observed in samples associated with air masses that did not pass over Southern South America suggest that local anthropogenic emissions were negligible. Thus the major source of non-crustal elements in aerosols over the study region may be long-range transport of aerosols from Southern Hemispheric continental regions containing a mixture of anthropogenic and crustal emissions.

3.2.3 Sea salt aerosol (Ca, Na^+, K^+)

The concentrations of sea-salt species were much higher than the other trace elements (Table 1). The concentrations of aerosol Ca were the highest among all elements measured in this study (range 16–53 ng m^{-3} and mean value of 30 ng m^{-3}). The mean value of Ca is close to the mean Ca concentrations observed previously in coastal regions of the Antarctic Peninsula (Artaxo et al., 1992; Weller et al., 2008) (Figure 4d). In addition, Na^+, as a tracer of sea-salt, and K^+, as a tracer of biomass burning (Zhu et al., 2015), were used to further evaluate the contribution of trace elements from other sources. The concentrations of Na^+ and K^+ showed average concentrations of 890 ± 310 and 28 ± 11 ng m^{-3}, respectively. Thus, the Na^+/K^+ (32 ± 3.5) ratios was close to the average Na/K mass ratio in seawater (27) and the Na^+/Ca ratios (31 ± 5.5) were close to the average Na^+/Ca ratio in seawater (26) as well (Millero, 2016). Such results agree well with the Na/K (29.7) and Na/Ca (39.9) ratios measured in snow samples collected at James Ross Island (Aristarain et al., 1982). Therefore, the Ca and K^+ in aerosols were derived primarily from sea salt at Palmer Station.

3.3 Aerosol particle-size distributions of trace elements

The concentrations of trace elements in aerosols observed during this study varied as a function of particle size. We applied k-means clustering to the full data set, and the results indicate that aerosol trace elements in the austral summer at Palmer Station can be classified into five groups based on their normalized particle size distributions (Figure 6), with each group showing a unique size distribution pattern: (1) crustal elements from crustal weathering and wind-induced resuspension of soil particles, (2) Al dominated by local minerals, (3) Pb from anthropogenic sources, as a result of long-range transport, (4) sea salt elements from the ocean, through bursting bubbles of seawater, and (5) P from local biogenic and soil resuspension. The particle size distribution of each element can be classified as single mode, bimodal, or trimodal, which hints that the elements derive from distinct sources or experienced different processes during the transport to the sampling site.

3.3.1 Single mode distribution

The particle size distributions of Na^+, P, K^+, Ca, Ti, and Ce showed a clear single coarse-mode distribution (Figure 7). As conservative species in seawater, Na^+, K^+, and Ca, were likely dominated by sea salt aerosols and all had a coarse primary mode at approximately 2.5 - 4.4 μm. Such a pattern agrees well with the particle size distributions of sea salt aerosols measured in coastal East Antarctica (Xu et al., 2013). Similarly, Ti and Ce derived from crustal emission were dominated by coarse-mode particles, peaking at around 4.4 μm. The aerosol P had a slightly shifted single mode distribution and peaked between the coarse-mode crustal aerosol and the sea salt aerosol at around 2.5 - 4.4 μm. Consequently, P was likely controlled by a regional emission source, such as soil resuspension. Given that gravitational settling greatly limits the residence time of coarse-mode particles compared with fine-mode particles, the elements with single coarse-mode distribution are likely to have a relatively proximal dominant source, such as the ice-free areas in the Antarctic Peninsula during austral summer.

3.3.2 Bimodal distribution

Although V and Mn also had a single mode distribution in most samples, bimodal distribution was found in a few samples, hinting at contributions from multiple sources (Figure 8). The particle size distribution of V and Mn primarily peaked around 4.4 μm while a small fine-mode peak could be seen around 0.14 - 0.25 μm in sample M2 and M4 for V, and a similar fine-mode peak also presented in M4 for Mn. A different Mn particle size distribution was dominated by particles larger than 18 μm, which is similar to Al and will be discussed below in section 3.3.3. As we concluded above, V and Mn were dominated by crustal emission and the coarse primary mode indicates regional crustal sources. As the size of dust particles decreases with distance away from the sources due to the higher deposition rates of coarse particles (Duce et al., 1991; Baker and Jickells, 2006). The fine-mode peaks are likely caused by additional input from long-range transport. The particle size distribution of V in M2 showed a unique peak in the fine-mode range. In addition, M2 had the highest concentrations of Ni and Cu among all the samples. The air mass back trajectories suggested a contribution from the South Pacific Ocean and coastal South America. This suggests that the fine-mode particles in M2 might be influenced by the remote anthropogenic emissions. By contrast, the air mass back trajectories for M4 directly passed the South American continent. An elevated Pb concentration and fine-mode peaks in Al and Pb size distributions were observed also in M4. Such results suggest M4 may have received polluted dust derived from South America.

3.3.3 Trimodal distribution

Aerosol Pb showed bimodal and trimodal distributions in this study (Figure 8). Comparing with the other elements, the primary mode of Pb was much finer and peaked at around 0.14 - 0.25 μm. The primary fine-mode fractions of aerosol Pb in some samples suggest that aerosol Pb at Palmer Station was occasionally dominated by anthropogenic sources as Pb is usually concentrated in fine particles from industrial or traffic emissions (Mamun et al., 2020). Air mass back trajectories also suggest the high Pb samples (M4, M5) received air mass derived from southern South America through long-range transport. The secondary mode of Pb was found around the same size as the crustal elements (approximately 4.4 μm), indicating a possible regional emission, including both crustal sources and local contaminated soil (Santos et al., 2005). In addition, a tertiary mode was observed in M4 and peaked around 0.78 - 1.4 μm. Considering M4 was influenced by long-range transport, Pb at this size range may be dominated by distinct remote sources. Thus Pb at Palmer Station was largely controlled by remote sources in South America. Because Pb was dominated by fine particles, an extremely small dry deposition velocity would be expected (Table 2). This might explain why previous studies in the Antarctic Peninsula suggested aerosol Pb was contributed by remote anthropogenic emission (Dick, 1991), whereas Pb in snow appeared to be associated with natural aerosols (Suttie and Wolff, 1992).

The average Al particle size distribution showed trimodal distribution with a primary mode at particle size larger than 18 μm, a secondary mode around 4.4 μm, and a tertiary mode around 0.14 - 0.25 μm (Figure 8). A single-mode Al particle size distribution peaked at around 4.4 μm which shared the same size with the primary mode of Ti, V, Mn, and Ce in sample M8

and M9, indicating the regional crustal emissions. Additional high peak (> 18 μm) was found in M1, M2, and M7 that contributed to bimodal distribution. A similar distribution can be seen in the Mn distribution of M2. We speculate that high Al concentrations associated with large particles might be caused by local soil resuspension around the sampling site, introducing large Al-containing particles that may come from aluminosilicate minerals. Such large Al-containing particles may not be unusual, as large-size dust particles were found in Antarctic snow (Winton et al., 2016). Trimodal distribution involved another mode in fine particles, approximately 0.14 - 0.25 μm, in M4 and M5. The high fine-mode Al of M4 and M5 likely derives from long-range transport from South America, which matches with the two highest Pb concentrations in this study.

3.3.4 Particle size distribution of mineral dust in Antarctica

Although the particle size distributions of crustal elements (Al, Ti, V, Mn, Ce) have been reported only rarely for Antarctica, the particle size distributions of mineral dust in aerosols, snow, and ice core samples were studied at several sites. The crustal aerosols sampled at Aboa research station, East Antarctica, had a single mode distribution peaking at particle size larger than 8.5 μm (Virkkula et al., 2006). In addition, the grain size distribution of dust particles in snow collected at Berkner Island was largely dominated by particles larger than 5 μm, suggesting a significantly higher proportion of dust was in coarse-mode than the previous size distribution observed at Kohnen Station, East Antarctic Plateau (Bory et al., 2010). Similarly, at Roosevelt Island, the particle size distributions of dust particles in snow were primarily dominated by coarse particles, possibly larger than 9 μm (Winton et al., 2016). Likewise, the dust particle size distribution in Dome C during the Last Glacial Maximum and the Holocene showed single-mode and peaked at approximately 2 - 3 μm in ice core samples (~3233 m above sea level) (Delmonte et al., 2002; Potenza et al., 2016). Therefore, the dust particle size distributions measured in coastal Antarctic regions are usually concentrated in coarse particles, whereas the dust particle size distributions of inland Antarctic regions, with longer pathways from the sources, show peaks in relatively finer particles.

3.4 Atmospheric dry deposition fluxes

Aerosol particle size distributions have been used to estimate atmospheric dry deposition fluxes of aerosol Fe to the Southern Ocean and coastal Antarctica (Gao et al., 2013; 2020). Similarly, the dry deposition fluxes of aerosol trace elements were estimated in this study (Table 3). Given that the sea-salt elements were the most abundant, Ca showed the highest dry deposition flux which varied from 0.59 to 6.6 mg m^{-2} yr^{-1} with an average of 1.2 ± 0.7 mg m^{-2} yr^{-1}. At the other extreme, due to low concentration and fine-mode particle dominance, aerosol Pb showed ~5000-fold lower dry deposition fluxes with a mean of 0.30 ± 0.23 μg m^{-2} yr^{-1}. The rough estimates of the dry deposition fluxes of Ni and Zn at Palmer Station are close to the median deposition fluxes found in the western North Atlantic Ocean (Ni: 18 μg m^{-2} yr^{-1}, Zn: 16 μg m^{-2} yr^{-1}), whereas the dry deposition flux of Cu is slightly higher than the median Zn dry deposition flux (2.8 μg m^{-2} yr^{-1}) in the western North Atlantic Ocean (Shelley et al., 2017). However, the dry deposition flux of Cu at Palmer Station is in the lower range of that observed in the eastern North Atlantic Ocean, 3.97 - 194 μg m^{-2} yr^{-1} (Buck et al., 2019). The estimated dry deposition fluxes of total continental dust at Palmer station ranged from 0.65 to 28 mg m^{-2} yr^{-1} with a mean of 5.5 ± 5.1 mg m^{-2} yr^{-1}, and this

fluxes is only around 10% of the mean global dust deposition flux at remote sites (Lawrence and Neff, 2009). Previous modelling studies estimated that wet deposition of dust through precipitation scavenging accounted for about 40~60% of the total deposition in the coastal and open oceans in the mid and low latitude oceans (Gao et al., 2003), and a similar wet deposition fraction was found in the Southern Ocean and coastal East Antarctica (Gao et al., 2013). Although precipitation varies in different regions, this is the best estimate we have for Antarctic regions. Assuming this wet deposition fraction (0.4-0.6) applies to the Antarctic Peninsula region, we approximate roughly a total dust flux of 10 ± 10 mg m^{-2} yr^{-1}. This value is at the lower end of the dust flux range, ~5 to ~50 mg m^{-2} yr^{-1}, estimated from ice core measurements at James Ross Island on the Antarctic Peninsula over the 20th century (McConnell et al., 2007), but it is higher than dust deposition flux at Dome C (0.2–0.6 mg m^{-2} yr^{-1}) (Lambert et al., 2012), at Talos Dome (0.70 - 7.24 mg m^{-2} yr^{-1}) (Albani et al., 2012) and the model estimate for this region (1.8–3.7 mg m^{-2} yr^{-1}) (Wagener et al., 2008). Considering active dust sources were reported at James Ross Island (Kavan et al., 2018), sites close to James Ross Island are likely to receive higher dust deposition fluxes. In addition, without measurements of wet deposition, the total dust deposition flux in our study could be underestimated. Comparing with the global data, the dust deposition flux at Palmer Station is far lower than the total dust deposition fluxes in the North and South Atlantic Ocean (minimum 270 and 150 mg m^{-2} yr^{-1}, respectively) (Barraqueta et al., 2019), the South Pacific Ocean (230 mg m^{-2} yr^{-1}) (Prospero, 1989), South Indian Ocean (240 mg m^{-2} yr^{-1}) (Heimburger et al., 2012) and McMurdo Dry Valleys (490 mg m^{-2} yr^{-1}) (Lancaster, 2002), while it is close to the estimated total dust deposition fluxes for the 63°S region (between 62°53'S and 63°53'S, along 170°6'W; 33 mg m^{-2} yr^{-1}) (Measures and Vink, 2000). Accordingly, the other crustal elements (P, Ti, V, Mn, Ce) were proportional to the dust dry deposition flux and showed extremely low values.

To examine the potential importance of atmospheric dust input to the particulate elemental concentrations in surface waters of the West Antarctic Peninsula shelf region, the maximum possible suspended particulate Al concentrations in surface seawater contributed by dust were estimated. We used the maximum Al dry deposition flux of 2300 μg m^{-2} yr^{-1} (Table 3), assumed that dry deposition accounted for 40% of total deposition (Gao et al., 2003) and assumed no settling loss from the mixed layer of mean depth 24 m (Eveleth et al., 2017) over a 4-month summer season. By this calculation, the accumulated concentration of suspended particulate Al contributed by total atmospheric deposition over this period is 3 nmol kg^{-1}. While suspended Al reaches 135 nmol kg^{-1} in coastal surface waters close to the peninsula, outer shelf and off-shelf surface waters generally have concentrations <5 nmol kg^{-1} (Annett et al., 2017), suggesting that this upper limit estimated dust flux could account for a substantial portion of observed surface ocean lithogenic particle concentration. While the mean Al flux is just 20% of this maximum, and settling loss from the mixed layer over the course of the summer may be significant, it is also possible that the residence time of particulate Al in the surface layer exceeds the summer season, by analogy to the North Atlantic (Jickells et al., 1999), allowing greater accumulation and concentrations than our simple calculation indicates. This rough estimate suggests that atmospheric dust deposition, possibly dominated by regional sources on the Antarctic continent itself, may contribute a significant fraction of suspended particulate concentrations of lithogenic elements in the surface waters of the outer shelf and the proximal pelagic Southern Ocean.

4 Conclusions and Implications

Results from this study indicate that trace elements in aerosols over Palmer Station during the austral summer were primarily derived from (1) the regional crustal sources, which includes P-enriched soil resuspension, (2) remote anthropogenic emissions in South America , and (3) seawater. Remote crustal sources and local contaminated soil may also contribute to aerosol trace elements at Palmer Station. The particle size distributions of crustal elements, including Al, P, Ti, V, Mn, and Ce, were all concentrated in coarse-mode, suggesting strong regional emissions likely from ice-free areas on the Antarctic Peninsula and its associated islands. In some samples, Al, V, and Mn also had a secondary peak in the fine-mode fraction, likely derived from a distinct source through long-range transport. We speculate that the modest enrichment of aerosol P over its crustal ratio to Al was caused by the resuspension of regional soils that are P-enriched as a result of the impact of nearby bird colonies. The elements Ca, Na^+, and K^+, had a single coarse-mode distribution, likely derived from sea-salt. Conversely, the size distribution of Pb occurred primarily in fine-mode. The airmass back trajectories show that samples with high concentrations of Ni, Cu, Zn and Pb were influenced by air masses passing through southern South America and the South Pacific Ocean. The total dust deposition flux (~10 mg m^{-2} yr^{-1}) during austral summer, estimated from the Al concentrations obtained in this study and an assumption of relative wet deposition, suggests that dust deposition plays a minor role in the concentrations of trace elements in coastal seawater around the West Antarctic Peninsula but may be more important in offshore regions. As the role of wet deposition is unquantified at present and remains poorly constrained for this region, the total deposition fluxes of trace elements during the austral summer could exceed the dry deposition fluxes reported here. Therefore, the importance of atmospheric deposition of trace elements to coastal West Antarctic Peninsula may need to be re-evaluated with additional observations of wet deposition. The Antarctic Peninsula is experiencing rapid climate change, with the expansion of ice-free areas and more frequent shipboard tourism with unknown impacts on aerosol chemistry in this region. To quantify future changes in in the atmospheric position and the impact in this region, long-term atmospheric observations of aerosol chemical and physical properties along with coupled studies of the ocean-atmosphere interactions would be needed.

Data availability. The data used in this paper has been submitted to the U.S. Antarctic Program Data Center (https://doi.org/10.15784/601370).

Author contributions. YG conceived the research. YG and SY prepared field sampling and collected aerosol samples. SF and YG digested samples. KB and RMS conducted sample analyses. SF wrote the 1st draft of the manuscript. YG and RMS edited the drafts. All authors contributed to writing and approved the submission.

Competing interests. The authors declare that they have no conflict of interest.

Acknowledgements. We thank Hugh Ducklow for encouragement of this research, Rafael Jusino-Atresino, Pami Mukherjee and Guojie Xu for participating in fieldwork preparation, and Jianqiong Zhan for assisting with meteorological data analyses. This work would not have become possible without the dedication and support from the staff of Palmer Station and the US Antarctic Program.

Financial support. The study was supported by the US NSF Grant 1341494 to YG.

References

Abram, N. J., Mulvaney, R., Wolff, E. W., Triest, J., Kipfstuhl, S., Trusel, L. D., Vimeux, F., Fleet, L., and Arrowsmith, C.: Acceleration of snow melt in an Antarctic Peninsula ice core during the twentieth century, Nature Geoscience, 6, 404, 2013.

Adebiyi, A. A., and Kok, J. F.: Climate models miss most of the coarse dust in the atmosphere, Science Advances, 6, eaaz9507, 2020.

Albani, S., Delmonte, B., Maggi, V., Baroni, C., Petit, J., Stenni, B., Mazzola, C., and Frezzotti, M.: Interpreting last glacial to Holocene dust changes at Talos Dome (East Antarctica): implications for atmospheric variations from regional to hemispheric scales, 2012.

Annett, A. L., Fitzsimmons, J. N., Séguret, M. J., Lagerström, M., Meredith, M. P., Schofield, O., and Sherrell, R. M.: Controls on dissolved and particulate iron distributions in surface waters of the Western Antarctic Peninsula shelf, Marine Chemistry, 196, 81-97, 2017.

Arimoto, R., Zeng, T., Davis, D., Wang, Y., Khaing, H., Nesbit, C., and Huey, G.: Concentrations and sources of aerosol ions and trace elements during ANTCI-2003, Atmospheric Environment, 42, 2864-2876, 2008.

Aristarain, A. J., Delmas, R. J., and Briat, M.: Snow chemistry on James Ross Island (Antarctic Peninsula), Journal of Geophysical Research: Oceans, 87, 11004-11012, 1982.

Artaxo, P., Andrade, F., and Maenhaut, W.: Trace elements and receptor modelling of aerosols in the Antarctic Peninsula, Nuclear Instruments and Methods in Physics Research Section B: Beam Interactions with Materials and Atoms, 49, 383-387, 1990.

Artaxo, P., Rabello, M. L., Maenhaut, W., and GRIEKEN, R. V.: Trace elements and individual particle analysis of atmospheric aerosols from the Antarctic Peninsula, Tellus B, 44, 318-334, 1992.

Artaxo, P., Oyola, P., and Martinez, R.: Aerosol composition and source apportionment in Santiago de Chile, Nuclear Instruments and Methods in Physics Research Section B: Beam Interactions with Materials and Atoms, 150, 409-416, 1999.

Asmi, E., Neitola, K., Teinilä, K., Rodriguez, E., Virkkula, A., Backman, J., Bloss, M., Jokela, J., Lihavainen, H., and De Leeuw, G.: Primary sources control the variability of aerosol optical properties in the Antarctic Peninsula, Tellus B: Chemical and Physical Meteorology, 70, 1-16, 2018.

Baker, A., and Jickells, T.: Mineral particle size as a control on aerosol iron solubility, Geophysical Research Letters, 33, 2006.

Baker, A. R., Li, M., and Chance, R.: Trace metal fractional solubility in size-segregated aerosols from the tropical eastern Atlantic Ocean, Global Biogeochemical Cycles, 34, e2019GB006510, 2020.

Barraqueta, J. L. M., Klar, J., Gledhill, M., Schlosser, C., Shelley, R., Planquette, H. F., Wenzel, B., Sarthou, G., and Achterberg, E.: Atmospheric deposition fluxes over the Atlantic Ocean: a GEOTRACES case study, Biogeosciences, 16, 1525-1542, 2019.

Blecker, S., Ippolito, J., Barrett, J., Wall, D., Virginia, R., and Norvell, K.: Phosphorus fractions in soils of Taylor Valley, Antarctica, Soil Science Society of America Journal, 70, 806-815, 2006.

Bockheim, J., Vieira, G., Ramos, M., López-Martínez, J., Serrano, E., Guglielmin, M., Wilhelm, K., and Nieuwendam, A.: Climate warming and permafrost dynamics in the Antarctic Peninsula region, Global and Planetary Change, 100, 215-223, 2013.

Boës, X., Rydberg, J., Martinez-Cortizas, A., Bindler, R., and Renberg, I.: Evaluation of conservative lithogenic elements (Ti, Zr, Al, and Rb) to study anthropogenic element enrichments in lake sediments, Journal of Paleolimnology, 46, 75-87, 2011.

Bollhöfer, A. F., Rosman, K. J. R., Dick, A. L., Chisholm, W., Burton, G. R., Loss, R. D., and Zahorowski, W.: Concentration, isotopic composition, and sources of lead in Southern Ocean air during 1999/2000, measured at the Cape Grim Baseline Air Pollution Station, Tasmania, Geochimica et Cosmochimica Acta, 69, 4747-4757, https://doi.org/10.1016/j.gca.2005.06.024, 2005.

Bory, A., Wolff, E., Mulvaney, R., Jagoutz, E., Wegner, A., Ruth, U., and Elderfield, H.: Multiple sources supply eolian mineral dust to the Atlantic sector of coastal Antarctica: Evidence from recent snow layers at the top of Berkner Island ice sheet, Earth and Planetary Science Letters, 291, 138-148, 2010.

Boutron, C., and Lorius, C.: Trace metals in Antarctic snows since 1914, Nature, 277, 551, 1979.

Bridgestock, L., Van De Flierdt, T., Rehkämper, M., Paul, M., Middag, R., Milne, A., Lohan, M. C., Baker, A. R., Chance, R., and Khondoker, R.: Return of naturally sourced Pb to Atlantic surface waters, Nature Communications, 7, 1-12, 2016.

Bromwich, D. H., Nicolas, J. P., Monaghan, A. J., Lazzara, M. A., Keller, L. M., Weidner, G. A., and Wilson, A. B.: Central West Antarctica among the most rapidly warming regions on Earth, Nature Geoscience, 6, 139, 2013.

Buck, C. S., Landing, W. M., and Resing, J. A.: Particle size and aerosol iron solubility: A high-resolution analysis of Atlantic aerosols, Marine Chemistry, 120, 14-24, 2010.

Buck, C. S., Aguilar-Islas, A., Marsay, C., Kadko, D., and Landing, W. M.: Trace element concentrations, elemental ratios, and enrichment factors observed in aerosol samples collected during the US GEOTRACES eastern Pacific Ocean transect (GP16), Chemical Geology, 511, 212-224, 2019.

Caliński, T., and Harabasz, J.: A dendrite method for cluster analysis, Communications in Statistics-theory and Methods, 3, 1-27, 1974.

Campbell, I. B., and Claridge, G.: Antarctica: soils, weathering processes and environment, Elsevier, 1987.

Carrasco, M. A., and Préndez, M.: Element distribution of some soils of continental Chile and the Antarctic peninsula. Projection to atmospheric pollution, Water, Air, and Soil Pollution, 57, 713-722, 1991.

Celo, V., Dabek-Zlotorzynska, E., and McCurdy, M.: Chemical characterization of exhaust emissions from selected Canadian marine vessels: the case of trace metals and lanthanoids, Environmental science & technology, 49, 5220-5226, 2015.

Chambers, S. D., Hong, S.-B., Williams, A. G., Crawford, J., Griffiths, A. D., and Park, S.-J.: Characterising terrestrial influences on Antarctic air masses using Radon-222 measurements at King George Island, Atmos Chem Phys, 14, 9903-9916, 2014.

Chen, Y.: Sources and fate of atmospheric nutrients over the remote oceans and their role on controlling marine diazotrophic microorganisms, 2004.

Chen, Y., and Siefert, R. L.: Seasonal and spatial distributions and dry deposition fluxes of atmospheric total and labile iron over the tropical and subtropical North Atlantic Ocean, Journal of Geophysical Research: Atmospheres, 109, 2004.

Chuang, P., Duvall, R., Shafer, M., and Schauer, J.: The origin of water soluble particulate iron in the Asian atmospheric outflow, Geophysical Research Letters, 32, 2005.

Cook, A. J., Holland, P., Meredith, M., Murray, T., Luckman, A., and Vaughan, D. G.: Ocean forcing of glacier retreat in the western Antarctic Peninsula, Science, 353, 283-286, 2016.

Crusius, J., Schroth, A. W., Gasso, S., Moy, C. M., Levy, R. C., and Gatica, M.: Glacial flour dust storms in the Gulf of Alaska: Hydrologic and meteorological controls and their importance as a source of bioavailable iron, Geophysical Research Letters, 38, 2011.

Delmonte, B., Petit, J., and Maggi, V.: Glacial to Holocene implications of the new 27000-year dust record from the EPICA Dome C (East Antarctica) ice core, Climate Dynamics, 18, 647-660, 2002.

Delmonte, B., Winton, H., Baroni, M., Baccolo, G., Hansson, M., Andersson, P., Baroni, C., Salvatore, M. C., Lanci, L., and Maggi, V.: Holocene dust in East Antarctica: Provenance and variability in time and space, The Holocene, 30, 546-558, 10.1177/0959683619875188, 2020.

Dick, A., and Peel, D.: Trace elements in Antarctic air and snowfall, Annals of Glaciology, 7, 12-19, 1985.

Dick, A.: Concentrations and sources of metals in the Antarctic Peninsula aerosol, Geochimica et cosmochimica acta, 55, 1827-1836, 1991.

Duce, R., Liss, P., Merrill, J., Atlas, E., Buat-Menard, P., Hicks, B., Miller, J., Prospero, J., Arimoto, R., and Church, T.: The atmospheric input of trace species to the world ocean, Global biogeochemical cycles, 5, 193-259, 1991.

Duce, R. A., and Tindale, N. W.: Atmospheric transport of iron and its deposition in the ocean, Limnology and oceanography, 36, 1715-1726, 1991.

Eveleth, R., Cassar, N., Sherrell, R., Ducklow, H., Meredith, M., Venables, H., Lin, Y., and Li, Z.: Ice melt influence on summertime net community production along the Western Antarctic Peninsula, Deep Sea Research Part II: Topical Studies in Oceanography, 139, 89-102, 2017.

Fomba, K., Müller, K., Van Pinxteren, D., and Herrmann, H.: Aerosol size-resolved trace metal composition in remote northern tropical Atlantic marine environment: case study Cape Verde islands, Atmos Chem Phys, 13, 4801, 2013.

Gantt, B., Hoque, S., Willis, R. D., Fahey, K. M., Delgado-Saborit, J. M., Harrison, R. M., Erdakos, G. B., Bhave, P. V., Zhang, K. M., and Kovalcik, K.: Near-road modeling and measurement of cerium-containing particles generated by nanoparticle diesel fuel additive use, Environmental science & technology, 48, 10607-10613, 2014.

Gao, Y., Fan, S., and Sarmiento, J.: Aeolian iron input to the ocean through precipitation scavenging: A modeling perspective and its implication for natural iron fertilization in the ocean, Journal of Geophysical Research: Atmospheres, 108, 2003.

Gao, Y., Xu, G., Zhan, J., Zhang, J., Li, W., Lin, Q., Chen, L., and Lin, H.: Spatial and particle size distributions of atmospheric dissolvable iron in aerosols and its input to the Southern Ocean and coastal East Antarctica, Journal of Geophysical Research: Atmospheres, 118, 12,634-612,648, 10.1002/2013jd020367, 2013.

Gao, Y., Marsay, C. M., Yu, S., Fan, S., Mukherjee, P., Buck, C. S., and Landing, W. M.: particle-Size Variability of Aerosol iron and impact on iron Solubility and Dry Deposition fluxes to the Arctic ocean, Scientific reports, 9, 1-11, 2019.

Gao, Y., Yu, S., Sherrell, R. M., Fan, S., Bu, K., and Anderson, J. R.: Particle-Size Distributions and Solubility of Aerosol Iron Over the Antarctic Peninsula During Austral Summer, Journal of Geophysical Research: Atmospheres, 125, e2019JD032082, 10.1029/2019jd032082, 2020.

Gras, J.: CN, CCN and particle size in Southern Ocean air at Cape Grim, Atmospheric research, 35, 233-251, 1995.

Guieu, C., Bonnet, S., Wagener, T., and Loÿe-Pilot, M. D.: Biomass burning as a source of dissolved iron to the open ocean?, Geophysical Research Letters, 32, 2005.

Heimburger, A., Losno, R., Triquet, S., Dulac, F., and Mahowald, N.: Direct measurements of atmospheric iron, cobalt, and aluminum-derived dust deposition at Kerguelen Islands, Global Biogeochemical Cycles, 26, 2012.

Herenz, P., Wex, H., Mangold, A., Laffineur, Q., Gorodetskaya, I. V., Fleming, Z. L., Panagi, M., and Stratmann, F.: CCN measurements at the Princess Elisabeth Antarctica research station during three austral summers, Atmospheric Chemistry & Physics, 19, 2019.

Hong, S., Kang, C. Y., and Kang, J.: Lichen Biomonitoring for the Detection of Local Heavy Metal Pollution around King Sejong Station, King George Island, Antarctica, 1999.

Järvinen, E., Virkkula, A., Nieminen, T., Aalto, P. P., Asmi, E., Lanconelli, C., Busetto, M., Lupi, A., Schioppo, R., and Vitale, V.: Seasonal cycle and modal structure of particle number size distribution at Dome C, Antarctica, Atmospheric Chemistry & Physics Discussions, 13, 2013.

Jasan, R., Plá, R., Invernizzi, R., and Dos Santos, M.: Characterization of atmospheric aerosol in Buenos Aires, Argentina, Journal of Radioanalytical and Nuclear Chemistry, 281, 101-105, 2009.

Jickells, T., and Moore, C. M.: The importance of atmospheric deposition for ocean productivity, Annual Review of Ecology, Evolution, and Systematics, 46, 481-501, 2015.

Jickells, T., Baker, A., and Chance, R.: Atmospheric transport of trace elements and nutrients to the oceans, Philosophical Transactions of the Royal Society A: Mathematical, Physical and Engineering Sciences, 374, 20150286, 2016.

Kaufman, Y. J., Tanré, D., and Boucher, O.: A satellite view of aerosols in the climate system, Nature, 419, 215-223, 2002.

Kavan, J., Dagsson-Waldhauserova, P., Renard, J.-B., Laska, K., and Ambrožová, K.: Aerosol concentrations in relationship to local atmospheric conditions on James Ross Island, Antarctica, 2018.

Keywood, M., Hibberd, M. F., Selleck, P. W., Desservettaz, M., Cohen, D. D., Stelcer, E., Atanacio, A. J., Scorgie, Y., and Tzu-Chi Chang, L.: Sources of Particulate Matter in the Hunter Valley, New South Wales, Australia, Atmosphere, 11, 4, 2020.

Kim, J., Yoon, Y. J., Gim, Y., Kang, H. J., Choi, J. H., Park, K.-T., and Lee, B. Y.: Seasonal variations in physical characteristics of aerosol particles at the King Sejong Station, Antarctic Peninsula, Atmos Chem Phys, 17, 12985-12999, 2017.

Klumpp, A., Domingos, M., and Pignata, M. L.: Air pollution and vegetation damage in South America—state of knowledge and perspectives, CRC Press LLC, United States of America, 2000.

Lachlan-Cope, T., Beddows, D. C., Brough, N., Jones, A. E., Harrison, R. M., Lupi, A., Jun Yoon, Y., Virkkula, A., and Dall'Osto, M.: On the annual variability of Antarctic aerosol size distributions at Halley Research Station, 2020.

Lambert, F., Bigler, M., Steffensen, J. P., Hutterli, M., and Fischer, H.: Centennial mineral dust variability in high-resolution ice core data from Dome C, Antarctica, Climate of the Past, 8, 609-623, 2012.

Lambert, G., Ardouin, B., and Sanak, J.: Atmospheric transport of trace elements toward Antarctica, Tellus B, 42, 76-82, 1990.

Lancaster, N.: Flux of eolian sediment in the McMurdo Dry Valleys, Antarctica: a preliminary assessment, Arctic, Antarctic, and Alpine Research, 34, 318-323, 2002.

Lawrence, C. R., and Neff, J. C.: The contemporary physical and chemical flux of aeolian dust: A synthesis of direct measurements of dust deposition, Chemical Geology, 267, 46-63, 2009.

Li, F., Ginoux, P., and Ramaswamy, V.: Distribution, transport, and deposition of mineral dust in the Southern Ocean and Antarctica: Contribution of major sources, Journal of Geophysical Research, 113, 10.1029/2007jd009190, 2008.

Loureiro, A., Vasconcellos, M., and Pereira, E.: Trace element determination in aerosols from the Antarctic Peninsula by neutron activation analysis, Journal of radioanalytical and nuclear chemistry, 159, 21-28, 1992.

Lowenthal, D. H., Chow, J. C., Mazzera, D. M., Watson, J. G., and Mosher, B. W.: Aerosol vanadium at McMurdo Station, Antarctica:: implications for Dye 3, Greenland, Atmospheric environment, 34, 677-679, 2000.

Lynch, H., Crosbie, K., Fagan, W., and Naveen, R.: Spatial patterns of tour ship traffic in the Antarctic Peninsula region, Antarctic Science, 22, 123-130, 2010.

Maenhaut, W., Zoller, W. H., Duce, R. A., and Hoffman, G. L.: Concentration and size distribution of particulate trace elements in the south polar atmosphere, Journal of Geophysical Research: Oceans, 84, 2421-2431, 1979.

Mahowald, N. M., Hamilton, D. S., Mackey, K. R., Moore, J. K., Baker, A. R., Scanza, R. A., and Zhang, Y.: Aerosol trace metal leaching and impacts on marine microorganisms, Nature communications, 9, 2614, 2018.

Mamun, A. A., Cheng, I., Zhang, L., Dabek-Zlotorzynska, E., and Charland, J.-P.: Overview of size distribution, concentration, and dry deposition of airborne particulate elements measured worldwide, Environmental Reviews, 28, 77-88, 2020.

Marsay, C. M., Kadko, D., Landing, W. M., Morton, P. L., Summers, B. A., and Buck, C. S.: Concentrations, provenance and flux of aerosol trace elements during US GEOTRACES Western Arctic cruise GN01, Chemical Geology, 502, 1-14, 2018.

Mazzera, D. M., Lowenthal, D. H., Chow, J. C., Watson, J. G., and Grubĭsíc, V.: PM10 measurements at McMurdo station, Antarctica, Atmospheric Environment, 35, 1891-1902, 2001.

McConnell, J. R., Aristarain, A. J., Banta, J. R., Edwards, P. R., and Simões, J. C.: 20th-Century doubling in dust archived in an Antarctic Peninsula ice core parallels climate change and desertification in South America, Proceedings of the National Academy of Sciences, 104, 5743-5748, 2007.

McConnell, J. R., Maselli, O. J., Sigl, M., Vallelonga, P., Neumann, T., Anschütz, H., Bales, R. C., Curran, M. A. J., Das, S. B., Edwards, R., Kipfstuhl, S., Layman, L., and Thomas, E. R.: Antarctic-wide array of high-resolution ice core records reveals pervasive lead pollution began in 1889 and persists today, Scientific Reports, 4, 5848, 10.1038/srep05848, 2014.

Measures, C., and Vink, S.: On the use of dissolved aluminum in surface waters to estimate dust deposition to the ocean, Global Biogeochemical Cycles, 14, 317-327, 2000.

Millero, F. J.: Chemical oceanography, CRC press, 2016.

Mishra, V. K., Kim, K.-H., Hong, S., and Lee, K.: Aerosol composition and its sources at the King Sejong Station, Antarctic peninsula, Atmospheric Environment, 38, 4069-4084, 2004.

Moore, C. M., Mills, M. M., Arrigo, K. R., Berman-Frank, I., Bopp, L., Boyd, P. W., Galbraith, E. D., Geider, R. J., Guieu, C., Jaccard, S. L., Jickells, T. D., La Roche, J., Lenton, T. M., Mahowald, N. M., Marañón, E., Marinov, I., Moore, J. K., Nakatsuka, T., Oschlies, A., Saito, M. A., Thingstad, T. F., Tsuda, A., and Ulloa, O.: Processes and patterns of oceanic nutrient limitation, Nature Geoscience, 6, 701-710, 10.1038/ngeo1765, 2013.

Mouri, H., Nagao, I., Okada, K., Koga, S., and Tanaka, H.: Elemental compositions of individual aerosol particles collected over the Southern Ocean: A case study, Atmospheric research, 43, 183-195, 1997.

Orr, A., Marshall, G. J., Hunt, J. C., Sommeria, J., Wang, C.-G., Van Lipzig, N. P., Cresswell, D., and King, J. C.: Characteristics of summer airflow over the Antarctic Peninsula in response to recent strengthening of westerly circumpolar winds, Journal of the Atmospheric Sciences, 65, 1396-1413, 2008.

Otero, X. L., De La Peña-Lastra, S., Pérez-Alberti, A., Ferreira, T. O., and Huerta-Diaz, M. A.: Seabird colonies as important global drivers in the nitrogen and phosphorus cycles, Nature Communications, 9, 246, 10.1038/s41467-017-02446-8, 2018.

Pacyna, J. M., and Pacyna, E. G.: An assessment of global and regional emissions of trace metals to the atmosphere from anthropogenic sources worldwide, Environmental reviews, 9, 269-298, 2001.

Pilinis, C., Pandis, S. N., and Seinfeld, J. H.: Sensitivity of direct climate forcing by atmospheric aerosols to aerosol size and composition, Journal of Geophysical Research: Atmospheres, 100, 18739-18754, 1995.

Potenza, M., Albani, S., Delmonte, B., Villa, S., Sanvito, T., Paroli, B., Pullia, A., Baccolo, G., Mahowald, N., and Maggi, V.: Shape and size constraints on dust optical properties from the Dome C ice core, Antarctica, Scientific reports, 6, 1-9, 2016.

Préndez, M., Wachter, J., Vega, C., Flocchini, R. G., Wakayabashi, P., and Morales, J. R.: PM2.5 aerosols collected in the Antarctic Peninsula with a solar powered sampler during austral summer periods, Atmospheric Environment, 43, 5575-5578, 10.1016/j.atmosenv.2009.07.030, 2009.

Prietzel, J., Prater, I., Hurtarte, L. C. C., Hrbáček, F., Klysubun, W., and Mueller, C. W.: Site conditions and vegetation determine phosphorus and sulfur speciation in soils of Antarctica, Geochimica et Cosmochimica Acta, 246, 339-362, 2019.

Prospero, J., Barrett, K., Church, T., Dentener, F., Duce, R., Galloway, J., Levy, H., Moody, J., and Quinn, P.: Atmospheric deposition of nutrients to the North Atlantic Basin, in: Nitrogen Cycling in the North Atlantic Ocean and its Watersheds, Springer, 27-73, 1996.

Prospero, J. M.: Mineral aerosol transport to the Pacific Ocean, Chemical oceanography, 10, 188-218, 1989.

Quinn, T., and Ondov, J.: Influence of temporal changes in relative humidity on dry deposition velocities and fluxes of aerosol particles bearing trace elements, Atmospheric Environment, 32, 3467-3479, 1998.

Rolph, G., Stein, A., and Stunder, B.: Real-time environmental applications and display sYstem: READY, Environmental Modelling & Software, 95, 210-228, 2017.

Saltzman, E. S.: Marine aerosols, Geophysical Monograph Series, 187, 17-35, 2009.

Santos, I. R., Silva-Filho, E. V., Schaefer, C. E., Albuquerque-Filho, M. R., and Campos, L. S.: Heavy metal contamination in coastal sediments and soils near the Brazilian Antarctic Station, King George Island, Marine pollution bulletin, 50, 185-194, 2005.

Shelley, R. U., Morton, P. L., and Landing, W. M.: Elemental ratios and enrichment factors in aerosols from the US-GEOTRACES North Atlantic transects, Deep Sea Research Part II: Topical Studies in Oceanography, 116, 262-272, 2015.

Shelley, R. U., Roca-Martí, M., Castrillejo, M., Sanial, V., Masqué, P., Landing, W. M., van Beek, P., Planquette, H., and Sarthou, G.: Quantification of trace element atmospheric deposition fluxes to the Atlantic Ocean (> 40 N; GEOVIDE, GEOTRACES GA01) during spring 2014, Deep Sea Research Part I: Oceanographic Research Papers, 119, 34-49, 2017.

Siefert, R. L., Johansen, A. M., and Hoffmann, M. R.: Chemical characterization of ambient aerosol collected during the southwest monsoon and intermonsoon seasons over the Arabian Sea: Labile-Fe (II) and other trace metals, Journal of Geophysical Research: Atmospheres, 104, 3511-3526, 1999.

Taylor, S. R., and McLennan, S. M.: The geochemical evolution of the continental crust, Reviews of geophysics, 33, 241-265, 1995.

Trabelsi, A., Masmoudi, M., Quisefit, J., and Alfaro, S.: Compositional variability of the aerosols collected on Kerkennah Islands (central Tunisia), Atmospheric research, 169, 292-300, 2016.

Tuncel, G., Aras, N. K., and Zoller, W. H.: Temporal variations and sources of elements in the South Pole atmosphere: 1. Nonenriched and moderately enriched elements, Journal of Geophysical Research: Atmospheres, 94, 13025-13038, 1989.

Turner, J., Barrand, N. E., Bracegirdle, T. J., Convey, P., Hodgson, D. A., Jarvis, M., Jenkins, A., Marshall, G., Meredith, M. P., and Roscoe, H.: Antarctic climate change and the environment: an update, Polar Record, 50, 237-259, 2014.

Van Lipzig, N., King, J., Lachlan-Cope, T., and Van den Broeke, M.: Precipitation, sublimation, and snow drift in the Antarctic Peninsula region from a regional atmospheric model, Journal of Geophysical Research: Atmospheres, 109, 2004.

Vaughan, D. G., Marshall, G. J., Connolley, W. M., Parkinson, C., Mulvaney, R., Hodgson, D. A., King, J. C., Pudsey, C. J., and Turner, J.: Recent rapid regional climate warming on the Antarctic Peninsula, Climatic change, 60, 243-274, 2003.

Viana, M., Amato, F., Alastuey, A. s., Querol, X., Moreno, T., García Dos Santos, S. l., Herce, M. D., and Fernández-Patier, R.: Chemical tracers of particulate emissions from commercial shipping, Environmental science & technology, 43, 7472-7477, 2009.

Viana, M., Hammingh, P., Colette, A., Querol, X., Degraeuwe, B., de Vlieger, I., and Van Aardenne, J.: Impact of maritime transport emissions on coastal air quality in Europe, Atmospheric Environment, 90, 96-105, 2014.

Virkkula, A., Teinilä, K., Hillamo, R., Kerminen, V. M., Saarikoski, S., Aurela, M., Koponen, I. K., and Kulmala, M.: Chemical size distributions of boundary layer aerosol over the Atlantic Ocean and at an Antarctic site, Journal of Geophysical Research: Atmospheres, 111, 2006.

Wagener, T., Guieu, C., Losno, R., Bonnet, S., and Mahowald, N.: Revisiting atmospheric dust export to the Southern Hemisphere ocean: Biogeochemical implications, Global Biogeochemical Cycles, 22, n/a-n/a, 10.1029/2007gb002984, 2008.

Warneck, P.: Chapter 7 The Atmospheric Aerosol, in: International Geophysics, edited by: Warneck, P., Academic Press, 278-373, 1988.

Weinzierl, B., Ansmann, A., Prospero, J., Althausen, D., Benker, N., Chouza, F., Dollner, M., Farrell, D., Fomba, W., and Freudenthaler, V.: The Saharan aerosol long-range transport and aerosol–cloud-interaction experiment: overview and selected highlights, Bulletin of the American Meteorological Society, 98, 1427-1451, 2017.

Weller, R., Wöltjen, J., Piel, C., Resenberg, R., Wagenbach, D., König-Langlo, G., and Kriews, M.: Seasonal variability of crustal and marine trace elements in the aerosol at Neumayer station, Antarctica, Tellus B: Chemical and Physical Meteorology, 60, 742-752, 2008.

Williams, R. M.: A model for the dry deposition of particles to natural water surfaces, Atmospheric Environment (1967), 16, 1933-1938, 1982.

Winton, V., Dunbar, G., Bertler, N., Millet, M. A., Delmonte, B., Atkins, C., Chewings, J., and Andersson, P.: The contribution of aeolian sand and dust to iron fertilization of phytoplankton blooms in southwestern Ross Sea, Antarctica, Global Biogeochemical Cycles, 28, 423-436, 2014.

Winton, V., Edwards, R., Delmonte, B., Ellis, A., Andersson, P., Bowie, A., Bertler, N., Neff, P., and Tuohy, A.: Multiple sources of soluble atmospheric iron to Antarctic waters, Global Biogeochemical Cycles, 30, 421-437, 2016.

Winton, V. H. L., Bowie, A. R., Edwards, R., Keywood, M., Townsend, A. T., van der Merwe, P., and Bollhöfer, A.: Fractional iron solubility of atmospheric iron inputs to the Southern Ocean, Marine Chemistry, 177, 20-32, 10.1016/j.marchem.2015.06.006, 2015.

Wu, J., and Boyle, E. A.: Lead in the western North Atlantic Ocean: completed response to leaded gasoline phaseout, Geochimica et Cosmochimica Acta, 61, 3279-3283, 1997.

Xu, G., Gao, Y., Lin, Q., Li, W., and Chen, L.: Characteristics of water-soluble inorganic and organic ions in aerosols over the Southern Ocean and coastal East Antarctica during austral summer, Journal of geophysical research: Atmospheres, 118, 13,303-313,318, 2013.

Xu, G., and Gao, Y.: Atmospheric trace elements in aerosols observed over the Southern Ocean and coastal East Antarctica, Polar Research, 33, 10.3402/polar.v33.23973, 2014.

Zhao, R., Han, B., Lu, B., Zhang, N., Zhu, L., and Bai, Z.: Element composition and source apportionment of atmospheric aerosols over the China Sea, Atmospheric Pollution Research, 6, 191-201, 2015.

Zhao, Y., and Gao, Y.: Mass size distributions of water-soluble inorganic and organic ions in size-segregated aerosols over metropolitan Newark in the US east coast, Atmospheric Environment, 42, 4063-4078, 2008.

Zhu, C., Kawamura, K., and Kunwar, B.: Effect of biomass burning over the western North Pacific Rim: wintertime maxima of anhydrosugars in ambient aerosols from Okinawa, Atmos Chem Phys, 15, 1959-1973, 2015.

Zhu, R., Kong, D., Sun, L., Geng, J., Wang, X., and Glindemann, D.: Tropospheric phosphine and its sources in coastal Antarctica, Environmental science & technology, 40, 7656-7661, 2006.

Zoller, W. H., Gladney, E., and Duce, R. A.: Atmospheric concentrations and sources of trace metals at the South Pole, Science, 183, 198-200, 1974.

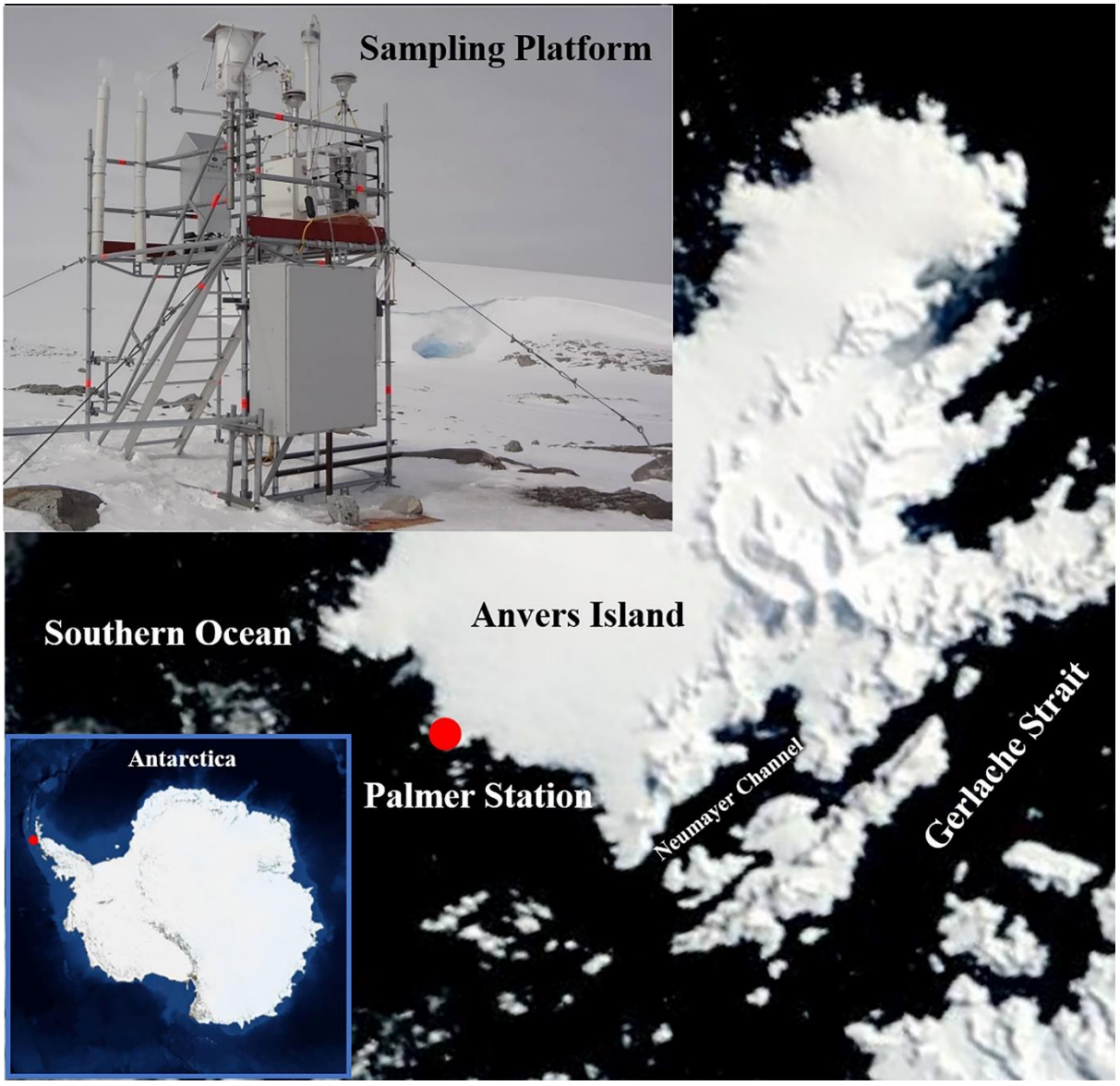

Figure 1: Sampling site at Palmer Station (red dot) with inset photograph of sampling platform (Gao et al., 2020) (satellite image credits: NASA).

735

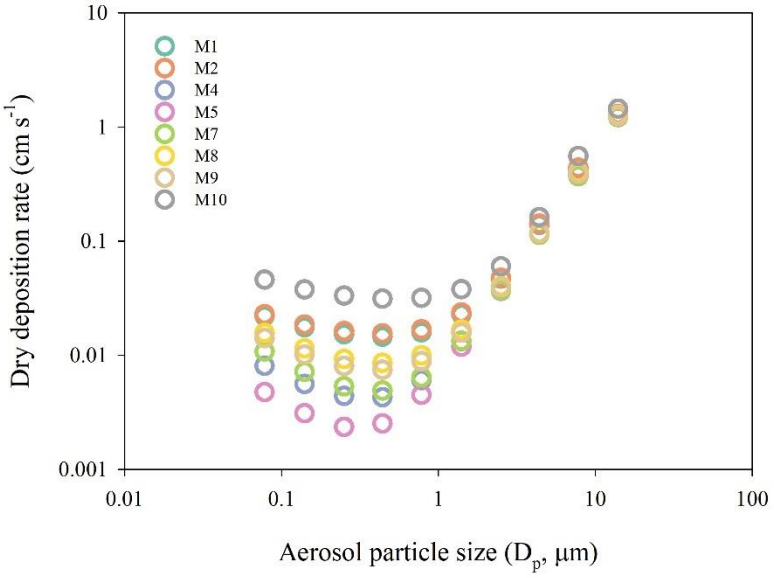

Figure 2: Median dry deposition rates of each size class of aerosol particles for samples M1-M10, collected between Nov 2016 and Jan 2017. The dry deposition rate is a function of aerosol particle size (Dp), but also depends on meteorological conditions (see text).

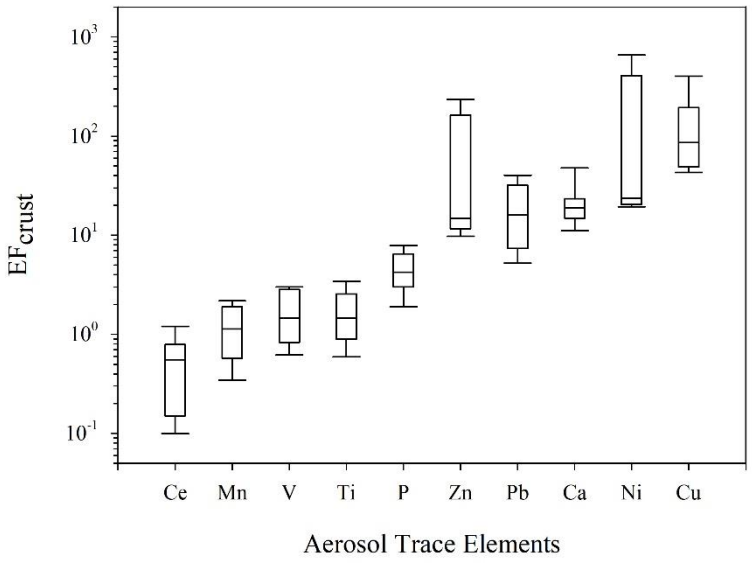

740

Figure 3: Box plots of EF_{crust} for trace elements in aerosols collected at Palmer Station between Nov 2016 and Jan 2017. The central horizontal line is the mean value, and the bottom and the top of each box are the 25th and 75th percentiles. The upper and lower horizontal bars indicate the 5th and 95th percentiles of the data.

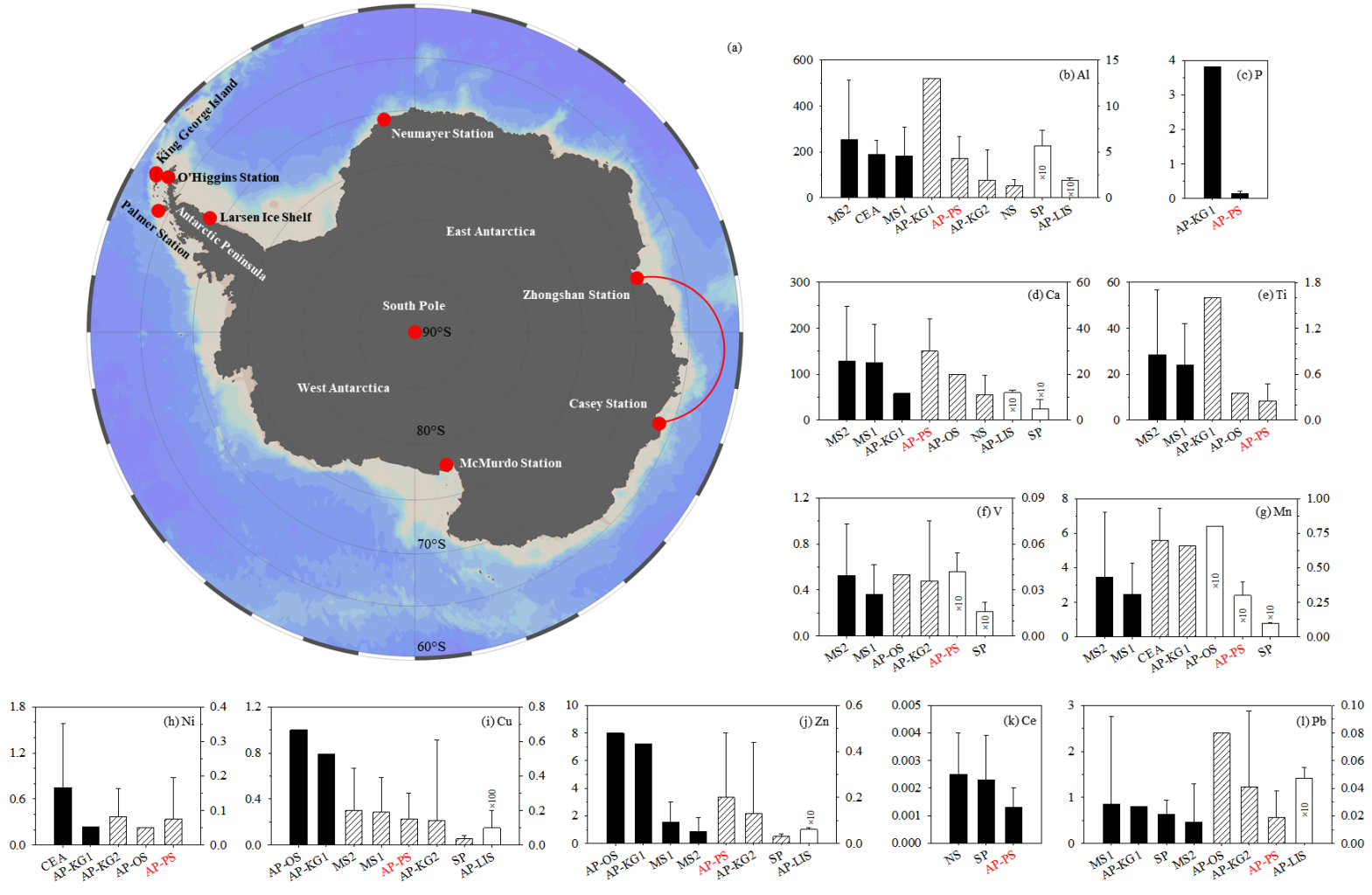

745 **Figure 4: Comparison of the concentrations of aerosol trace elements (ng m^{-3}) over Antarctica at coastal land-based sites. The cruise from Zhongshan Station to Casey Station was used to represent coastal East Antarctica. All concentrations are sorted in descending order from left to right. The left y-axis shows concentrations for the black bars, whereas the right y-axis corresponds to the striped and white bars. Some extremely low values are multiplied by 10 or 100 for display purposes, as marked above the corresponding white bars. Error bars show the standard derivation of the trace element concentrations in each study if available. Data are from**
750 **observations conducted at South Pole (SP) (Zoller et al., 1974), Hut Point site (MS1, PM_{10}) and Radar Sat Dome site (MS2, PM_{10}) at McMurdo Station (Mazzera et al., 2001), on a cruise between Zhongshan Station and Casey Station in the Coastal East Antarctica (CEA) (Xu and Gao, 2014), at Neumayer Station (NS) (Weller et al., 2008), and at 5 sites on the Antarctic Peninsula (AP), including Comandante Ferraz Antarctic Station (KG1) (Artaxo et al., 1990; Artaxo et al., 1992) and King Sejong Station (KG2) (Mishra et al., 2004) at King George Island, O'Higgins Station (OS, $PM_{2.5}$) (Préndez et al., 2009), Larsen Ice Shelf (LIS) (Dick, 1991), and Palmer**
755 **Station (PS, this study, marked by red arrow) at Anvers Island. Artaxo et al. (1990); Artaxo et al. (1992); Mazzera et al. (2001), and**

Préndez et al. (2009) used X-ray fluorescence to measure the total concentrations of trace elements. All the other studies applied acid digestion methods. Our study at Palmer Station is marked in red.

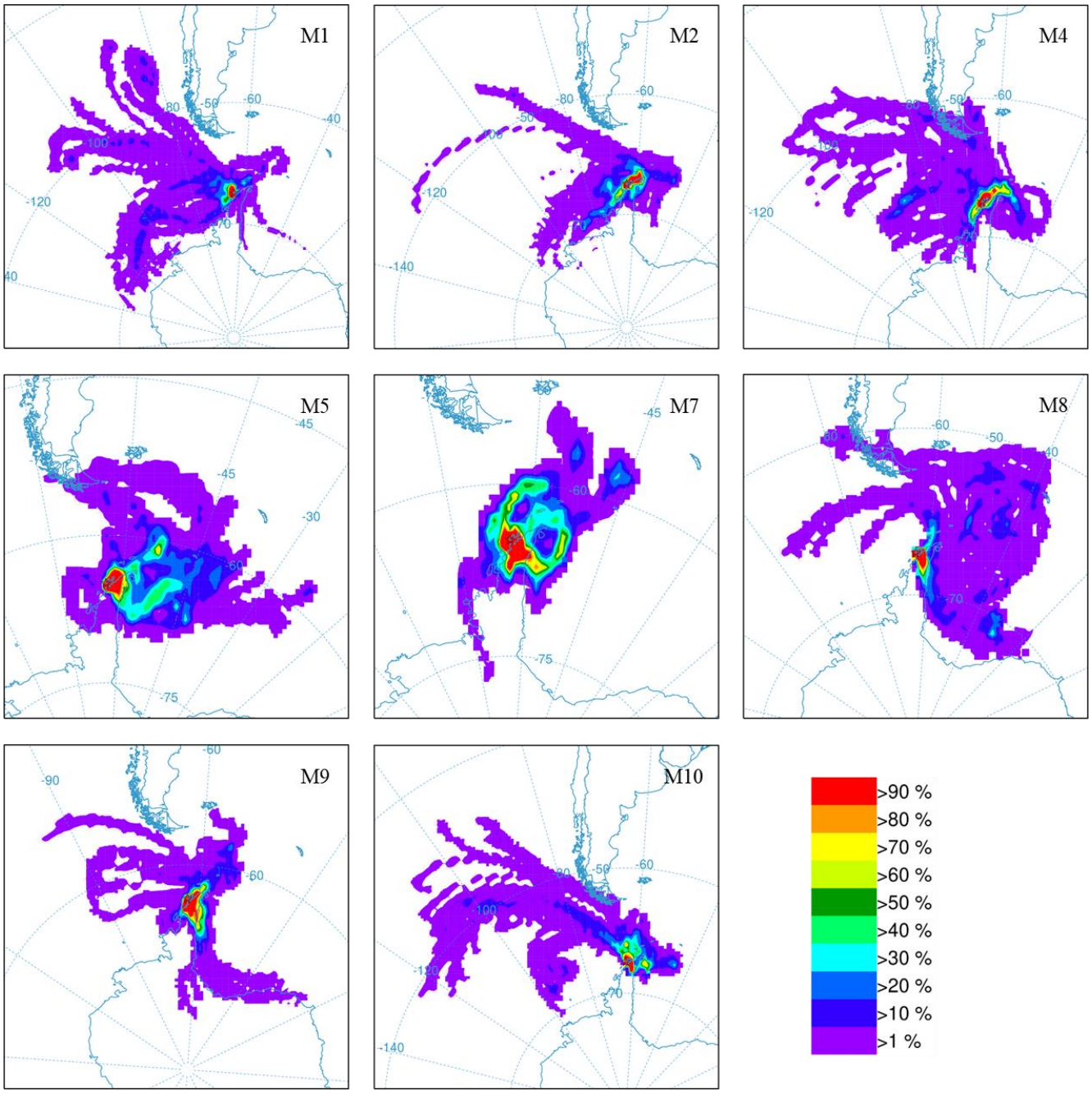

760

Figure 5: Frequencies of 72-hour air mass back trajectories for samples collected at Palmer Station: M1 (Nov 19 – Nov 26, 2016), M2 (Nov 26 – Dec 4, 2016), M4 (Dec 09 – Dec 17, 2016), M5 (Dec 17 – Dec 24, 2016), M7 (Jan 1 – Jan 8, 2017), M8 (Jan 8 – Jan 15, 2017), M9 (Jan 15 – Jan 23, 2017), and M10 (Jan 23 – Jan 30, 2017).

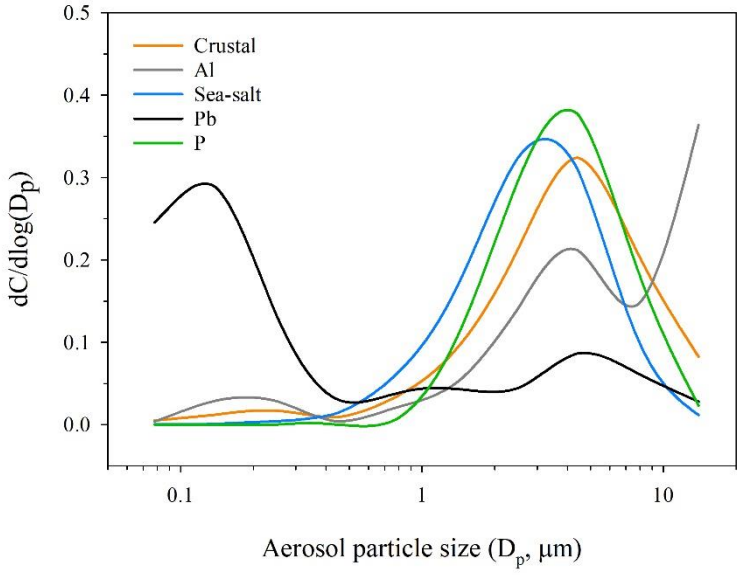

765

Figure 6. The results of k-means clustering on the normalized mean aerosol particle size distributions. The crustal cluster includes Ti, V, Mn, Ce and the sea-salt cluster includes Na^+, K^+, Ca.

770

775

780

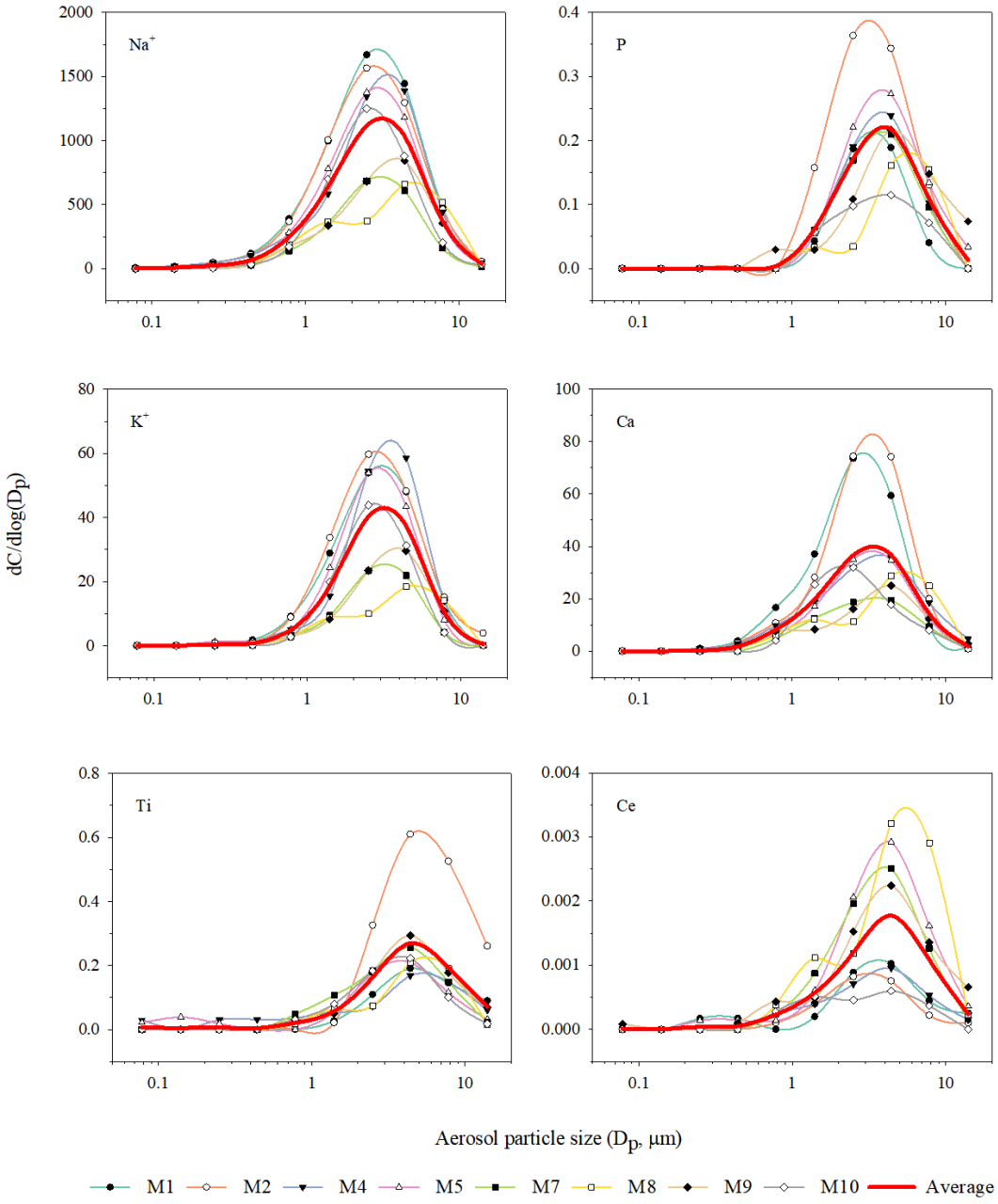

785 **Figure 7: Particle size distributions of the trace elements showing single-mode distribution in aerosols during Nov 2016 – Jan 2017 austral summer over Palmer Station. dC/dlog(D_p) is the normalized concentration.**

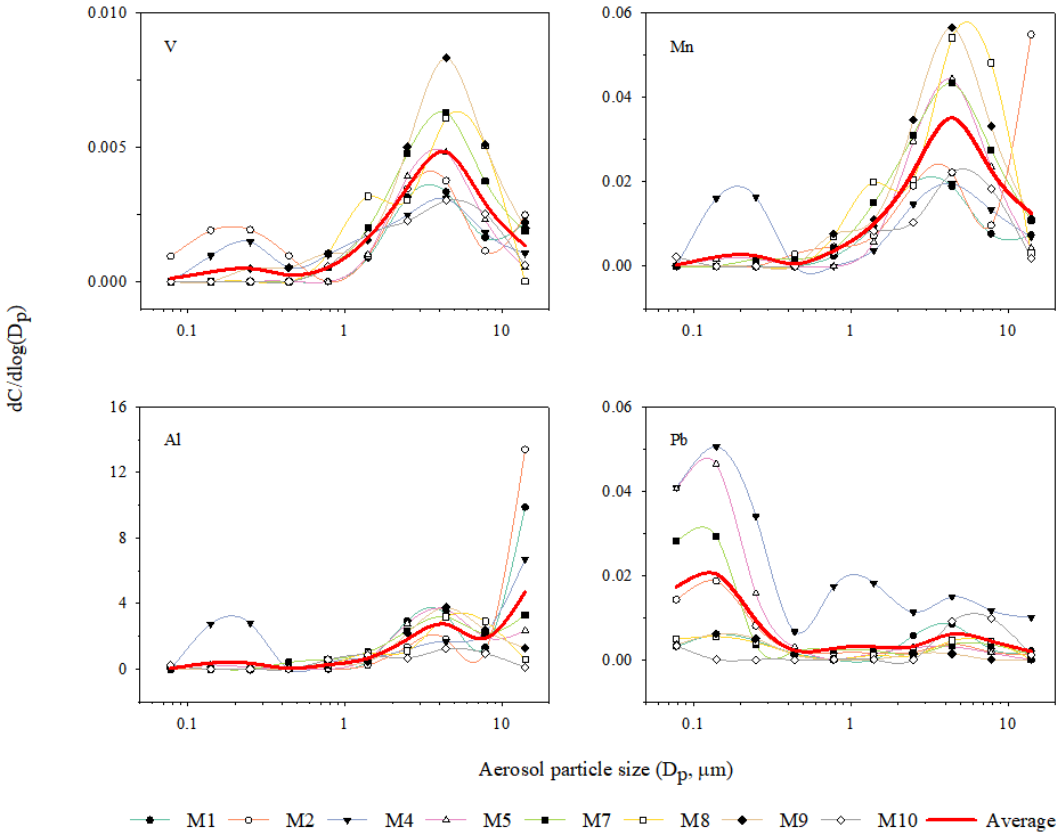

Figure 8: Particle size distributions of the trace elements showing bimodal and trimodal distribution in aerosols during Nov 2016 – Jan 2017 austral summer over Palmer Station. dC/dlog(D_p) is the normalized concentration.

Table 1. Sampling periods and meteorological conditions for individual samples (Gao et al. 2020).

Sample ID	Sampling Period	%Actual Sampling Time* (%)	Sampling Volume (m^3)	Wind Speed ($m\ s^{-1}$)	Air Temperature (^oC)	Relative Humidity (%)	Air Pressure (hPa)	Precip. ($mm\ d^{-1}$)	Solar Intensity ($W\ m^{-2}$)
M1	11/19/2016-11/26/2016	78	225	5.7 (0.7-22)	0.1 (-2.2-4.3)	87 (52-100)	990 (976-1011)	4.19	166 (0-675)
M2	11/26/2016-12/04/2016	71	233	4.9 (0.4-21)	0.7 (-2.2-5.8)	82 (45-100)	982 (959-997)	1.37	191 (0-847)
M4	12/09/2016-12/17/2016	80	266	3.5 (0.1-15)	0.7 (-3.3-5.6)	83 (53-100)	985 (969-998)	0.37	207 (1-854)
M5	12/17/2016-12/24/2016	88	264	2.5 (0.3-9.8)	2.0 (-0.7-5.5)	77 (49-100)	988 (972-996)	0.05	195 (1-723)
M7	01/01/2017-01/08/2017	85	244	4.1 (0.2-13)	1.8 (-0.7-3.8)	72 (49-99)	987 (972-997)	0.09	272 (0-857)
M8	01/08/2017-01/15/2017	94	283	5.4 (0.7-16)	2.6 (0.3-5.5)	64 (46-95)	982 (973-991)	0	225 (0-792)
M9	01/15/2017-01/23/2017	87	285	5.0 (0.2-15)	2.1 (-1.0-5.3)	65 (42-86)	987 (981-997)	0.15	260 (0-829)
M10	01/23/2017-01/30/2017	98	279	8.9 (0.7-21)	4.1 (1.7-7.1)	79 (65-90)	981 (969-997)	3.7	110 (0-594)

*Actual sampling time / total sampling time × 100%

Table 2. Concentrations of trace elements and ions in aerosols over Palmer Station, West Antarctic Peninsula.

Element/Ion	Units	Size Fraction	M1	M2	M4	M5	M7	M8	M9	M10	Mean	S.D
Al	ng m^{-3}	Coarse	6.9	7.9	4.4	3.3	3.7	2.2	2.5	0.83	4.0	2.4
		Fine	ND	ND	1.6	0.13	0.30	0.11	0.17	0.41	0.34	0.53
		Sum	6.9	7.9	6.0	3.4	4.0	2.3	2.7	1.2	4.3	2.4
P	pg m^{-3}	Coarse	110	250	150	180	130	95	140	85	140	53
		Fine	ND	ND	ND	ND	ND	ND	15	ND	1.9	5.3
		Sum	110	250	150	180	130	95	160	85	150	54
Ca	ng m^{-3}	Coarse	42	47	25	24	14	18	15	20	26	12
		Fine	8.9	5.4	5.4	3.2	2.4	3.1	3.9	2.0	4.3	2.2
		Sum	50	53	31	27	16	21	19	22	30	14
Ti	pg m^{-3}	Coarse	150	800	120	150	170	130	190	94	230	230
		Fine	ND	ND	48	20	24	9.0	16	65	23	23
		Sum	150	800	170	170	190	140	210	160	250	220
V	pg m^{-3}	Coarse	3.2	3.6	2.4	3.1	4.8	4.1	5.3	2.4	3.6	1.1
		Fine	ND	1.4	1.2	ND	0.27	0.53	0.77	0.28	0.57	0.55
		Sum	3.2	5.0	3.7	3.1	5.0	4.6	6.1	2.7	4.2	1.2
Mn	pg m^{-3}	Coarse	17	42	15	27	32	34	35	14	27	10
		Fine	1.2	2.3	8.2	0.90	2.9	3.6	3.9	2.8	3.2	2.3
		Sum	18	44	23	27	35	38	39	17	30	10
Ni	pg m^{-3}	Coarse	ND	320	ND	17	23	ND	ND	ND	45	110
		Fine	37	ND	ND	ND	ND	ND	ND	200	30	70
		Sum	37	320	ND	17	23	ND	ND	200	75	120
Cu	pg m^{-3}	Coarse	170	200	17	ND	ND	ND	ND	120	63	86
		Fine	69	280	92	52	110	ND	36	34	84	86
		Sum	240	480	110	52	110	ND	36	150	150	150
Zn	pg m^{-3}	Coarse	40	68	32	590	280	25	ND	46	140	200
		Fine	51	ND	30	120	300	ND	ND	56	70	100
		Sum	90	68	61	710	580	25	ND	100	200	280
Ce	pg m^{-3}	Coarse	0.73	0.57	0.62	1.8	1.6	2.1	1.5	0.41	1.2	0.65
		Fine	0.084	0.051	0.12	0.13	0.12	0.19	0.26	0.14	0.14	0.064
		Sum	0.81	0.62	0.74	2.0	1.7	2.2	1.8	0.55	1.3	0.69

Pb	pg m^{-3}	Coarse	5.1	2.4	13.8	2.2	2.4	2.7	0.70	5.0	4.3	4.1
		Fine	3.8	12	46	28	17	4.5	4.3	1.7	15	16
		Sum	9.0	14	60	30	19	7.2	5.0	6.6	19	19
Na^+	ng m^{-3}	Coarse	1100	1000	900	870	430	450	520	730	749	260
		Fine	220	210	160	120	75	99	89	90	130	57
		Sum	1300	1200	1100	1000	510	550	610	820	890	310
K^+	ng m^{-3}	Coarse	34	39	34	31	14	12	17	24	26	10
		Fine	4.9	4.5	2.5	3.2	1.6	1.8	1.5	1.4	2.3	1.1
		Sum	39	43	37	34	15	14	19	25	28	11

795

Table 3. Estimates of dry deposition velocities and dry deposition fluxes of trace elements in aerosols over Palmer Station, West Antarctic Peninsula.

	Element	Velocity (cm s^{-1})		Flux (μg m^{-2} yr^{-1})	
		Range	Mean	Range	Mean
	Dust			650-28000	5500±5100
EF<10	Al	0.14-1.6	0.49	52-2300	440±410
	P	0.092-0.52	0.17	3.3-33	7.5±4.4
	Ti	0.14-0.92	0.27	7.1-120	18±15
	V	0.14-0.85	0.26	0.16-0.77	0.32±0.11
	Mn	0.18-1.1	0.28	0.94-11	2.5±1.6
	Ce	0.10-0.65	0.20	0.017-0.31	0.084±0.048
EF>10	Ca	0.073-0.41	0.13	580-6600	1200±660
	Pb	0.0097-0.83	0.11	0.018-1.5	0.30±0.23
	Ni*		0.11-0.49	3.9-17	
	Cu*		0.11-0.49	6.0-25	
	Zn*		0.11-0.49	8.1-36	

*The range of dry deposition fluxes of Ni, Cu, and Zn was estimated based on Pb and Al dry deposition velocities, discussed in the text.